TMD Effects in Polarized Processes Phenomenology Overview

Transversity 2024 – Trieste – 03-07 June 2024

Francesco Murgia
INFN – Sezione di Cagliari - Italy

Outline

- TMDs: Physical motivation, definitions
- TMD factorization, evolution, resummation: SIDIS, DY and e+e- annihilation
- Theoretical information: bounds, sum rules
- Phenomenology: Sivers and Boer-Mulders functions, Collins and polarizing FFs
- Phenomenology: worm-gears, pretzelosity [gluon Sivers TMD]
- Related topics not covered: gluon TMDs, GTMDs and quarkonium (talks by D. Boer and S. Bhattacharya), subleading twist contributions (talk by S. Rodini), HSO approach (talk by T. Rogers), SCET (talk by I. Scimemi), Lattice QCD (talk by C. Alexandrou)
- Future (EIC, LHC, LHCSpin, AMBER, SoLID,JLab20+,...)

TMD Handbook Arxiv: 230403302 [hep-ph]

TMDs and friends

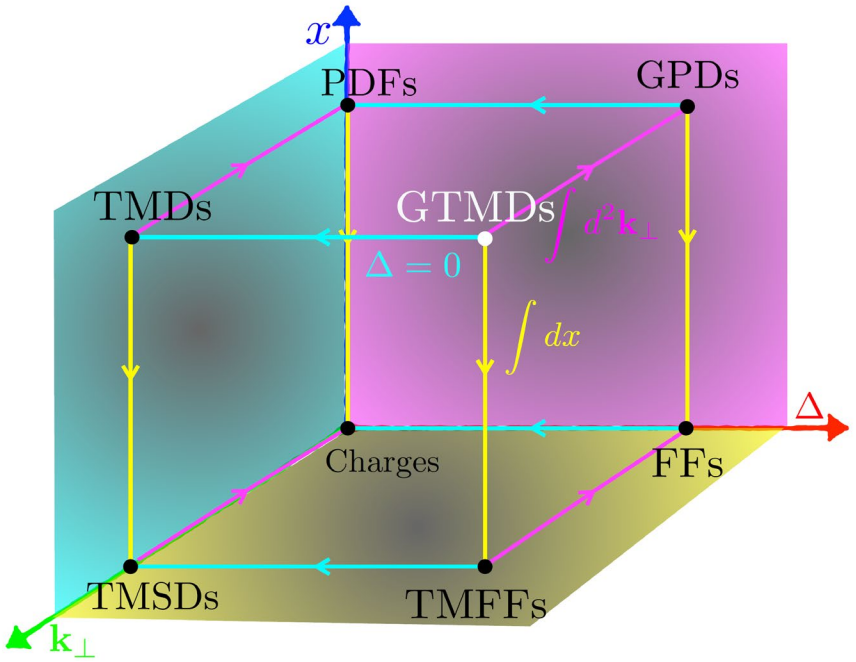

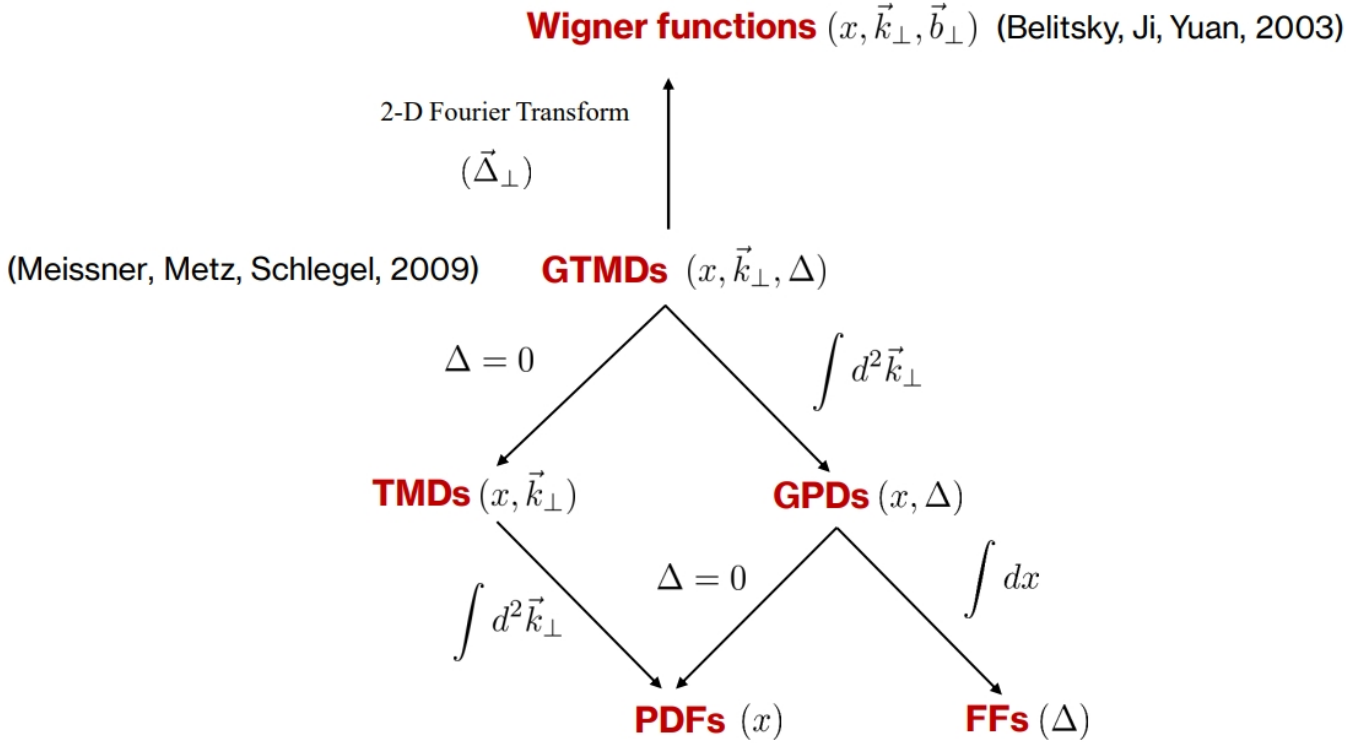

Historical recollections

- **Studies of TMD effects in parton model date back to its formulation – low transverse momentum spectra in unpolarized DY processes**
- **TSSAs (and hyperon transverse polarization) in pp, pA collisions, Sivers effect, generalized parton model, problems with T-odd TMDs, factorization**
- **Initial and final state interactions in SIDIS, DY and e+e- collisions, gauge links, factorization, modified universality [sign change of T-odd Sivers and BM functions between SIDIS and DY]**
- **Proper formulation of TMD factorization theorems at leading power, rapidity divergences, TMD evolution (CSS, SCET)**
- **Resummation (low q_T) vs fixed-order (large $q_T \sim Q$), matching, connection with collinear twist-3 approach**

TMD Factorization and evolution (CSS formalism) basic ideas and ingredients

(for more details see talk by L. Rossi on Thursday)
(SCET approach see talk by I. Scimemi on Thursday)

- Fourier transform to b_T space
- Renormalize ultraviolet and rapidity divergences
- RG evolution equations with proper anomalous dimensions (Kollins-Soper kernel for rapidity)
- Avoid large b_T regime and Landau pole in perturbative expansion (b_* prescription)
- Perform OPE to evolve from the initial to the final (b_* implemented) scales
- Require nonperturbative input for CS kernel [$g_K(b_T^2)$] and for the OPE part
- The nonperturbative factor at the initial Q_0 scale effectively incorporates also the soft factor S

$$\hat{f}_1^a(x, \boldsymbol{b}_T^2; \mu_f, \zeta_f)$$
$$= [C \otimes f_1](x, b_*; \mu_{b_*}, \mu_{b_*}^2) \exp\left\{ \int_{\mu_{b_*}}^{\mu_f} \frac{d\mu}{\mu} \gamma(\mu, \zeta_f) \right\} \left(\frac{\zeta_f}{\mu_{b_*}^2} \right)^{K(b_*, \mu_{b_*})/2} f_{1NP}(x, \boldsymbol{b}_T^2; \zeta_f, Q_0),$$

TMD Factorization and evolution (CSS formalism) basic ideas and ingredients

Phenomenological approaches differ in the choice of required ingredients:

- Order of perturbative expansion in the strong coupling costant (LO, NLO, NNLO, N3LO)
- Order in the resummation of large logarithms (LL, NLL, NNLL, N3LL, N4LL)
- Parametrization of nonperturbative input: $g_K(b_T^2)$, functional form of distributions at the initial scale (e.g. combinations of Gaussians and weighted Gaussians, flavor dependence, …)
- Choice of data sets to be fitted for SIDIS, DY, e+e- annihilation, pp collisions…
- Data selection criteria for the validity of the factorization approach (safe kinematical regions)
- Choice of collinear PDFs and FFs
- Evaluation of statistical uncertainty bands
- ….

Leading Quark TMDPDFs

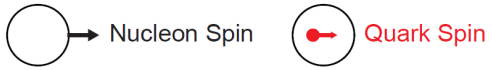

Nucleon Polarization	Quark Polarization: Un-Polarized (U)	Quark Polarization: Longitudinally Polarized (L)	Quark Polarization: Transversely Polarized (T)
U	f_1 = Unpolarized		$h_1^\perp$ = Boer-Mulders
L		g_1 = Helicity	$h_{1L}^\perp$ = Worm-gear
T	$f_{1T}^\perp$ = Sivers	$g_{1T}^\perp$ = Worm-gear	h_1 = Transversity; $h_{1T}^\perp$ = Pretzelosity

Leading Quark TMDFFs

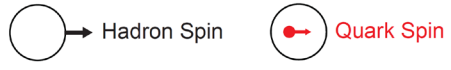

	Quark Polarization: Un-Polarized (U)	Quark Polarization: Longitudinally Polarized (L)	Quark Polarization: Transversely Polarized (T)
Unpolarized (or Spin 0) Hadrons	D_1 = Unpolarized		$H_1^\perp$ = Collins
Polarized Hadrons: L		G_1 = Helicity	$H_{1L}^\perp$
Polarized Hadrons: T	$D_{1T}^\perp$ = Polarizing FF	$G_{1T}^\perp$	H_1 = Transversity; $H_{1T}^\perp$

Leading Gluon TMDPDFs

Nucleon Spin — Gluon Operator Helicities

Nucleon Polarization	Gluon Operator Polarization: Un-Polarized	Helicity 0 antisymmetric	Helicity 2
U	f_1^g = ● Unpolarized		$h_1^{\perp g}$ = ↑●↑ + ↓●↓ Linearly Polarized
L		g_{1L}^g = ↑●↓ → − ↓●↑ → Helicity	$h_{1L}^{\perp g}$ = → + →
T	$f_{1T}^{\perp g}$ = ● − ●	$g_{1T}^{\perp g}$ = → − ←	h_{1T}^g = ↑●↑ + ↓●↓ Transversity $h_{1T}^{\perp g}$ = → + ←

Leading Gluon TMDFFs

Hadron Spin — Gluon Operator Helicities

		Gluon Operator Polarization: Un-Polarized	Helicity 0 antisymmetric	Helicity 2
Unpolarized (or Spin 0) Hadrons		D_1^g = ● Unpolarized		$H_1^{\perp g}$ = ↑●↑ + ↓●↓ Linearly Polarized
Polarized Hadrons	L		G_{1L}^g = ↑●↓ → − ↓●↑ → Helicity	$H_{1L}^{\perp g}$ = → + →
	T	$D_{1T}^{\perp g}$ = ● − ●	$G_{1T}^{\perp g}$ = → − ←	H_{1T}^g = ↑●↑ + ↓●↓ Transversity $H_{1T}^{\perp g}$ = → + ←

Subleading Quark-Gluon-Quark TMDPDFs

		Quark Chirality	
		Chiral Even	Chiral Odd
Nucleon Polarization	U	$\tilde{f}^{\perp}, \tilde{g}^{\perp}$	$\tilde{e}\ ,\ \tilde{h}$
	L	$\tilde{f}_L^{\perp}, \tilde{g}_L^{\perp}$	$\tilde{e}_L, \tilde{h}_L$
	T	$\tilde{f}_T, \tilde{f}_T^{\perp}, \tilde{g}_T, \tilde{g}_T^{\perp}$	$\tilde{e}_T, \tilde{e}_T^{\perp}, \tilde{h}_T, \tilde{h}_T^{\perp}$

Subleading Quark-Gluon-Quark TMDFFs

		Quark Chirality	
		Chiral Even	Chiral Odd
Unpolarized (or Spin 0) Hadrons		$\tilde{D}^{\perp},\ \tilde{G}^{\perp}$	$\tilde{E}\ ,\ \tilde{H}$
Polarized Hadrons	L	$\tilde{D}_L^{\perp}, \tilde{G}_L^{\perp}$	$\tilde{E}_L, \tilde{H}_L$
	T	$\tilde{D}_T, \tilde{D}_T^{\perp}, \tilde{G}_T, \tilde{G}_T^{\perp}$	$\tilde{E}_T, \tilde{E}_T^{\perp}, \tilde{H}_T, \tilde{H}_T^{\perp}$

TMD PDFs for spin-1 hadrons (up to twist 4)

TABLE II. List of twist-2 quark TMDs for a spin-1 hadron in terms of the quark and hadron polarizations. The square brackets [ ] indicate chiral-odd distributions and the others are chiral-even ones.

	Quark					
	U(γ^+)		L($\gamma^+\gamma_5$)		T($i\sigma^{i+}\gamma_5/\sigma^{i+}$)	
Hadron	T-even	T-odd	T-even	T-odd	T-even	T-odd
U	f_1					$[h_1^\perp]$
L			g_{1L}		$[h_{1L}^\perp]$	
T		$f_{1T}^\perp$	g_{1T}		$[h_1], [h_{1T}^\perp]$	
LL	f_{1LL}					$[h_{1LL}^\perp]$
LT	f_{1LT}			g_{1LT}		$[h_{1LT}], [h_{1LT}^\perp]$
TT	f_{1TT}			g_{1TT}		$[h_{1TT}], [h_{1TT}^\perp]$

TABLE IV. List of twist-3 quark TMDs for a spin-1 hadron in terms of the hadron polarizations and the operator forms in the correlation functions. The square brackets [] indicate chiral-odd distributions and the others are chiral-even ones. The LL, LT, and TT TMDs are new distributions found in this work.

	Quark					
Hadron	$\gamma^i, 1, i\gamma_5$		$\gamma^+\gamma_5$		σ^{ij}, σ^{-+}	
	T-even	T-odd	T-even	T-odd	T-even	T-odd
U	$f^\perp[e]$			$g^\perp$		$[h]$
L		$f_L^\perp[e_L]$	$g_L^\perp$		$[h_L]$	
T		$f_T, f_T^\perp[e_T, e_T^\perp]$	$g_T, g_T^\perp$		$[h_T], [h_T^\perp]$	
LL	$f_{LL}^\perp[e_{LL}]$			$g_{LL}^\perp$		$[h_{LL}]$
LT	$f_{LT}, f_{LT}^\perp[e_{LT}, e_{LT}^\perp]$			$g_{LT}, g_{LT}^\perp$		$[h_{LT}], [h_{LT}^\perp]$
TT	$f_{TT}, f_{TT}^\perp[e_{TT}, e_{TT}^\perp]$			$g_{TT}, g_{TT}^\perp$		$[h_{TT}], [h_{TT}^\perp]$

Bacchetta, Mulders - PRD 62, 114004 (2000)
Kumano, Song - PRD 103, 014025 (2021)

Formal constraints on TMDs

Notice: These constraints are formally valid for bare TMDs with partonic interpretation, not clear if they are preserved for renormalized TMDs. Useful for test models and for phenomenology.

Positivity constraints [Bacchetta, Boglione, Henneman, Mulders, PRL 85, 712 (2000)]

$$f_1^a(x,k_T) \geq 0\ , \quad |g_1^a(x,k_T)| \leq f_1^a(x,k_T)\ , \quad |h_1^a(x,k_T)| \leq f_1^a(x,k_T)$$

$$|h_1^a(x,k_T)| \leq \frac{1}{2}\left(f_1^a(x,k_T) + g_1^a(x,k_T)\right)$$

$$|h_{1T}^{\perp(1)a}(x,k_T)| \leq \frac{1}{2}\left(f_1^a(x,k_T) - g_1^a(x,k_T)\right)$$

$$g_{1T}^{\perp(1)a}(x,k_T)^2 + f_{1T}^{\perp(1)a}(x,k_T)^2 \leq \frac{k_T^2}{4M_N^2}\left(f_1^a(x,k_T)^2 - g_1^a(x,k_T)^2\right)$$

$$h_{1L}^{\perp(1)a}(x,k_T)^2 + h_1^{\perp(1)a}(x,k_T)^2 \leq \frac{k_T^2}{4M_N^2}\left(f_1^a(x,k_T)^2 - g_1^a(x,k_T)^2\right)$$

Formal constraints on TMDs

Burkardt sum rule for the Sivers function [Burkardt, PRD 69 091501 (2004)]

$$\sum_a \int dx \int d^2k_T \, f_{1T}^{\perp(1)a}(x, k_T) = 0$$

Schäfer-Teryaev sum rule for the Collins FF [Schäfer, Teryaev, PRD 61 077903 (2000)]

$$\sum_h (2S_h + 1) \int dz \, z \int d^2K_T \, H_1^{\perp(1)q/h}(z, K_T) = 0$$

Semi-Inclusive DIS

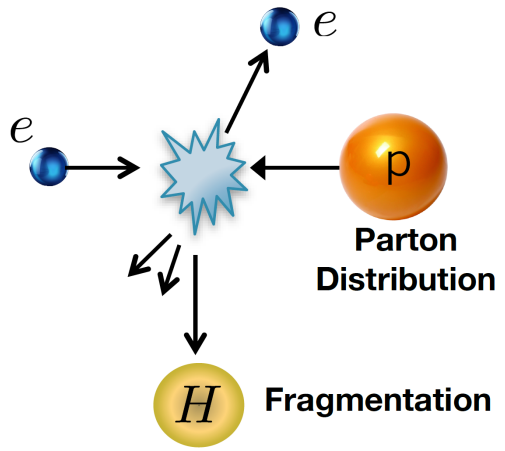

Drell-Yan

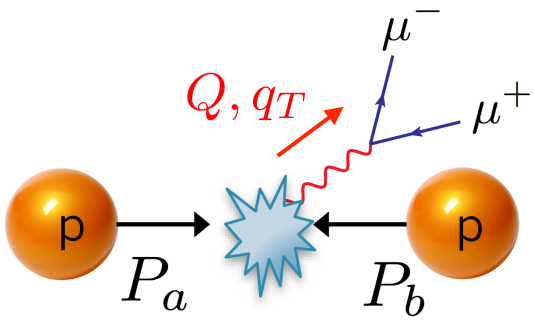

$$q_T \ll Q$$

Dihadron in e^+e^-

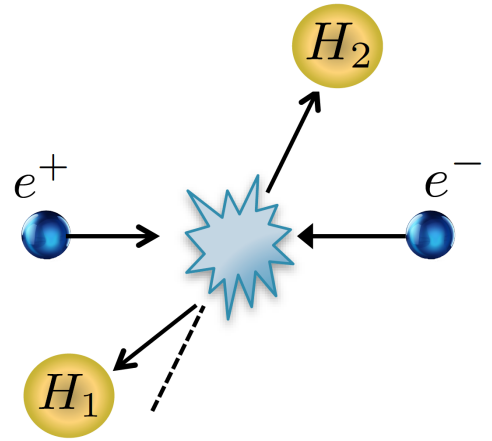

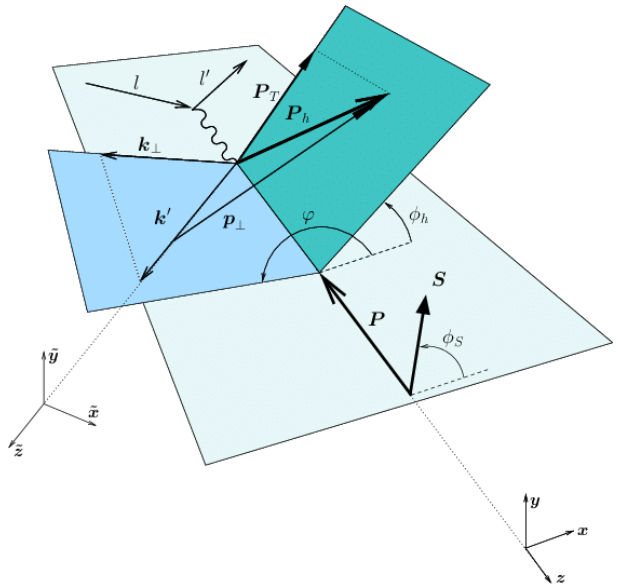

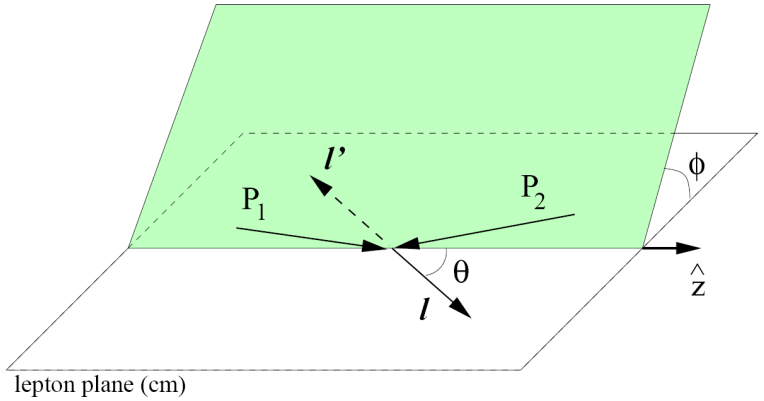

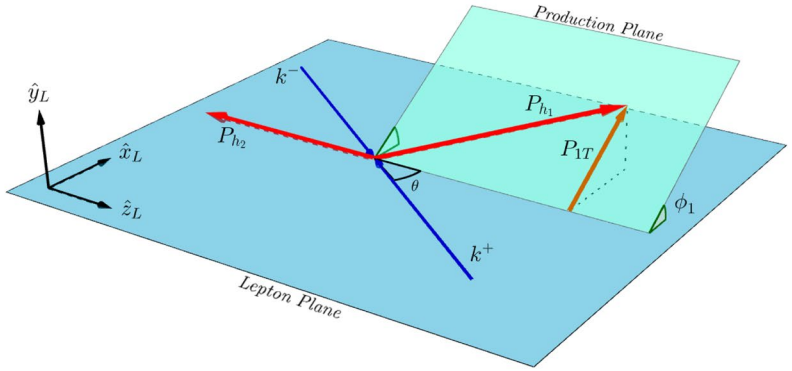

SIDIS cross section

$$\frac{d\sigma}{dx\,dy\,d\psi\,dz\,d\phi_h\,dP_{h\perp}^2} =$$

$$\frac{\alpha^2}{xyQ^2}\,\frac{y^2}{2\,(1-\varepsilon)}\left(1+\frac{\gamma^2}{2x}\right)\Big\{F_{UU,T}+\varepsilon F_{UU,L}+\sqrt{2\,\varepsilon(1+\varepsilon)}\,\cos\phi_h\,F_{UU}^{\cos\phi_h}$$

Boer-Mulders,Cahn,...

$$+\,\varepsilon\cos(2\phi_h)\,F_{UU}^{\cos 2\phi_h}+\lambda_e\sqrt{2\,\varepsilon(1-\varepsilon)}\,\sin\phi_h\,F_{LU}^{\sin\phi_h}$$

$$+\,S_\parallel\left[\sqrt{2\,\varepsilon(1+\varepsilon)}\,\sin\phi_h\,F_{UL}^{\sin\phi_h}+\varepsilon\sin(2\phi_h)\,F_{UL}^{\sin 2\phi_h}\right]$$

Worm-gear $h_{1L}^\perp$

$$+\,S_\parallel\lambda_e\left[\sqrt{1-\varepsilon^2}\,F_{LL}+\sqrt{2\,\varepsilon(1-\varepsilon)}\,\cos\phi_h\,F_{LL}^{\cos\phi_h}\right]$$

Sivers

$$+\,|\boldsymbol{S}_\perp|\left[\sin(\phi_h-\phi_S)\left(F_{UT,T}^{\sin(\phi_h-\phi_S)}+\varepsilon\,F_{UT,L}^{\sin(\phi_h-\phi_S)}\right)\right.$$

Collins

$$+\,\varepsilon\,\sin(\phi_h+\phi_S)\,F_{UT}^{\sin(\phi_h+\phi_S)}+\varepsilon\,\sin(3\phi_h-\phi_S)\,F_{UT}^{\sin(3\phi_h-\phi_S)}$$

Pretzelosity $h_{1T}^\perp$

$$\left.+\,\sqrt{2\,\varepsilon(1+\varepsilon)}\,\sin\phi_S\,F_{UT}^{\sin\phi_S}+\sqrt{2\,\varepsilon(1+\varepsilon)}\,\sin(2\phi_h-\phi_S)\,F_{UT}^{\sin(2\phi_h-\phi_S)}\right]$$

Worm-gear $g_{1T}^\perp$

$$+\,|\boldsymbol{S}_\perp|\lambda_e\left[\sqrt{1-\varepsilon^2}\,\cos(\phi_h-\phi_S)\,F_{LT}^{\cos(\phi_h-\phi_S)}+\sqrt{2\,\varepsilon(1-\varepsilon)}\,\cos\phi_S\,F_{LT}^{\cos\phi_S}\right.$$

$$\left.\left.+\,\sqrt{2\,\varepsilon(1-\varepsilon)}\,\cos(2\phi_h-\phi_S)\,F_{LT}^{\cos(2\phi_h-\phi_S)}\right]\right\},$$

Bacchetta et al, JHEP 02 (2007) 093

Drell-Yan cross section for dilepton production

$$\frac{d\sigma}{d^4q d\Omega} = \frac{\alpha_{\rm em}^2}{Fq^2}\{((1+\cos^2\theta)F_{UU}^1 + (1-\cos^2\theta)F_{UU}^2 + \sin 2\theta\cos\phi F_{UU}^{\cos\phi} + \sin^2\theta\cos 2\phi F_{UU}^{\cos 2\phi})$$

Boer-Mulders

$$+ S_{aL}(\sin 2\theta\sin\phi F_{LU}^{\sin\phi} + \sin^2\theta\sin 2\phi F_{LU}^{\sin 2\phi}) + S_{bL}(\sin 2\theta\sin\phi F_{UL}^{\sin\phi} + \sin^2\theta\sin 2\phi F_{UL}^{\sin 2\phi})$$

Worm-gear $h_{1L}^{\perp}$ & BM

Sivers

$$+ |\vec{S}_{aT}|[\sin\phi_a((1+\cos^2\theta)F_{TU}^1 + (1-\cos^2\theta)F_{TU}^2 + \sin 2\theta\cos\phi F_{TU}^{\cos\phi} + \sin^2\theta\cos 2\phi F_{TU}^{\cos 2\phi})$$
$$+ \cos\phi_a(\sin 2\theta\sin\phi F_{TU}^{\sin\phi} + \sin^2\theta\sin 2\phi F_{TU}^{\sin 2\phi})] + |\vec{S}_{bT}|[\sin\phi_b((1+\cos^2\theta)F_{UT}^1 + (1-\cos^2\theta)F_{UT}^2$$
$$+ \sin 2\theta\cos\phi F_{UT}^{\cos\phi} + \sin^2\theta\cos 2\phi F_{UT}^{\cos 2\phi}) + \cos\phi_b(\sin 2\theta\sin\phi F_{UT}^{\sin\phi} + \sin^2\theta\sin 2\phi F_{UT}^{\sin 2\phi})]$$
$$+ S_{aL}S_{bL}((1+\cos^2\theta)F_{LL}^1 + (1-\cos^2\theta)F_{LL}^2 + \sin 2\theta\cos\phi F_{LL}^{\cos\phi} + \sin^2\theta\cos 2\phi F_{LL}^{\cos 2\phi})$$
$$+ S_{aL}|\vec{S}_{bT}|[\cos\phi_b((1+\cos^2\theta)F_{LT}^1 + (1-\cos^2\theta)F_{LT}^2 + \sin 2\theta\cos\phi F_{LT}^{\cos\phi} + \sin^2\theta\cos 2\phi F_{LT}^{\cos 2\phi})$$
$$+ \sin\phi_b(\sin 2\theta\sin\phi F_{LT}^{\sin\phi} + \sin^2\theta\sin 2\phi F_{LT}^{\sin 2\phi})] + |\vec{S}_{aT}|S_{bL}[\cos\phi_a((1+\cos^2\theta)F_{TL}^1 + (1-\cos^2\theta)F_{TL}^2$$
$$+ \sin 2\theta\cos\phi F_{TL}^{\cos\phi} + \sin^2\theta\cos 2\phi F_{TL}^{\cos 2\phi}) + \sin\phi_a(\sin 2\theta\sin\phi F_{TL}^{\sin\phi} + \sin^2\theta\sin 2\phi F_{TL}^{\sin 2\phi})]$$
$$+ |\vec{S}_{aT}||\vec{S}_{bT}|[\cos(\phi_a+\phi_b)((1+\cos^2\theta)F_{TT}^1 + (1-\cos^2\theta)F_{TT}^2 + \sin 2\theta\cos\phi F_{TT}^{\cos\phi} + \sin^2\theta\cos 2\phi F_{TT}^{\cos 2\phi})$$
$$+ \cos(\phi_a-\phi_b)((1+\cos^2\theta)\bar{F}_{TT}^1 + (1-\cos^2\theta)\bar{F}_{TT}^2 + \sin 2\theta\cos\phi\bar{F}_{TT}^{\cos\phi} + \sin^2\theta\cos 2\phi\bar{F}_{TT}^{\cos 2\phi})$$
$$+ \sin(\phi_a+\phi_b)(\sin 2\theta\sin\phi F_{TT}^{\sin\phi} + \sin^2\theta\sin 2\phi F_{TT}^{\sin 2\phi})$$
$$+ \sin(\phi_a-\phi_b)(\sin 2\theta\sin\phi\bar{F}_{TT}^{\sin\phi} + \sin^2\theta\sin 2\phi\bar{F}_{TT}^{\sin 2\phi})]\}.$$

Arnold, Metz, Schlegel
PRD 79, 034005 (2009)

Back-to-back hadron pair production in e+e- annihilation

$$
\begin{aligned}
4\frac{P_a^0 P_b^0 d\sigma_{em}}{d^3\vec{P}_a d^3\vec{P}_b} = \frac{\alpha_{em}^2}{q^4}\{\{&[(1+\cos^2\theta)F_{UU}^1 + (1-\cos^2\theta)F_{UU}^3 + (\sin 2\theta\cos\phi)F_{UU}^{\cos\phi} + (\sin^2\theta\cos 2\phi)F_{UU}^{\cos 2\phi}] \\
&+ \Lambda_a[(\sin^2\theta\sin 2\phi)F_{LU}^{\sin 2\phi} + (\sin 2\theta\sin\phi)F_{LU}^{\sin\phi}] \\
&+ |\vec{S}_{a\perp}|[\sin\phi_a((1+\cos^2\theta)F_{TU}^1 + (1-\cos^2\theta)F_{TU}^3 + (\sin 2\theta\cos\phi)F_{TU}^{\cos\phi} + (\sin^2\theta\cos 2\phi)F_{TU}^{\cos 2\phi}) \\
&+ \cos\phi_a((\sin^2\theta\sin 2\phi)F_{TU}^{\sin 2\phi} + (\sin 2\theta\sin\phi)F_{TU}^{\sin\phi})] + \Lambda_b[(\sin^2\theta\sin 2\phi)F_{UL}^{\sin 2\phi} + (\sin 2\theta\sin\phi)F_{UL}^{\sin\phi}] \\
&+ |\vec{S}_{b\perp}|[\sin\phi_b((1+\cos^2\theta)F_{UT}^1 + (1-\cos^2\theta)F_{UT}^3 + (\sin 2\theta\cos\phi)F_{UT}^{\cos\phi} + (\sin^2\theta\cos 2\phi)F_{UT}^{\cos 2\phi}) \\
&+ \cos\phi_b((\sin^2\theta\sin 2\phi)F_{UT}^{\sin 2\phi} + (\sin 2\theta\sin\phi)F_{UT}^{\sin\phi})] \\
&+ \Lambda_a\Lambda_b[(1+\cos^2\theta)F_{LL}^1 + (1-\cos^2\theta)F_{LL}^3 + (\sin 2\theta\cos\phi)F_{LL}^{\cos\phi} + (\sin^2\theta\cos 2\phi)F_{LL}^{\cos 2\phi}] \\
&+ \Lambda_a|\vec{S}_{b\perp}|[\cos\phi_b((1+\cos^2\theta)F_{LT}^1 + (1-\cos^2\theta)F_{LT}^3 + (\sin 2\theta\cos\phi)F_{LT}^{\cos\phi} \\
&+ (\sin^2\theta\cos 2\phi)F_{LT}^{\cos 2\phi}) + \sin\phi_b((\sin^2\theta\sin 2\phi)F_{LT}^{\sin 2\phi} + (\sin 2\theta\sin\phi)F_{LT}^{\sin\phi})] \\
&+ |\vec{S}_{a\perp}|\Lambda_b[\cos\phi_a((1+\cos^2\theta)F_{TL}^1 + (1-\cos^2\theta)F_{TL}^3 + (\sin 2\theta\cos\phi)F_{TL}^{\cos\phi} \\
&+ (\sin^2\theta\cos 2\phi)F_{TL}^{\cos 2\phi}) + \sin\phi_a((\sin^2\theta\sin 2\phi)F_{TL}^{\sin 2\phi} + (\sin 2\theta\sin\phi)F_{TL}^{\sin\phi})] \\
&+ |\vec{S}_{a\perp}||\vec{S}_{b\perp}|[\cos(\phi_a+\phi_b)((1+\cos^2\theta)F_{TT}^1 + (1-\cos^2\theta)F_{TT}^3 \\
&+ (\sin 2\theta\cos\phi)F_{TT}^{\cos\phi} + (\sin^2\theta\cos 2\phi)F_{TT}^{\cos 2\phi}) + \cos(\phi_a-\phi_b)((1+\cos^2\theta)\bar{F}_{TT}^1 + (1-\cos^2\theta)\bar{F}_{TT}^3 \\
&+ (\sin 2\theta\cos\phi)\bar{F}_{TT}^{\cos\phi} + (\sin^2\theta\cos 2\phi)\bar{F}_{TT}^{\cos 2\phi}) + \sin(\phi_a+\phi_b)((\sin^2\theta\sin 2\phi)F_{TT}^{\sin 2\phi} + (\sin 2\theta\sin\phi)F_{TT}^{\sin\phi}) \\
&+ \sin(\phi_a-\phi_b)((\sin^2\theta\sin 2\phi)\bar{F}_{TT}^{\sin 2\phi} + (\sin 2\theta\sin\phi)\bar{F}_{TT}^{\sin\phi})]\} - 2\lambda_e\{[(\sin\theta\sin\phi)G_{UU}^{\sin\phi}] \\
&+ \Lambda_a[(\cos\theta)G_{LU}^2 + (\sin\theta\cos\phi)G_{LU}^{\cos\phi}] \\
&+ |\vec{S}_{a\perp}|[\cos\phi_a((\cos\theta)\bar{G}_{TU}^2 + (\sin\theta\cos\phi)G_{TU}^{\cos\phi}) + \sin\phi_a((\sin\theta\sin\phi)G_{TU}^{\sin\phi})] \\
&+ \Lambda_b[(\cos\theta)G_{UL}^2 + (\sin\theta\cos\phi)G_{UL}^{\cos\phi}] \\
&+ |\vec{S}_{b\perp}|[\cos\phi_b((\cos\theta)\bar{G}_{UT}^2 + (\sin\theta\cos\phi)G_{UT}^{\cos\phi}) + \sin\phi_b((\sin\theta\sin\phi)G_{UT}^{\sin\phi})] \\
&+ \Lambda_a\Lambda_b[(\sin\theta\sin\phi)G_{LL}^{\sin\phi}] + \Lambda_a|\vec{S}_{b\perp}|[\cos\phi_b((\sin\theta\sin\phi)G_{LT}^{\sin\phi}) + \sin\phi_b((\cos\theta)\bar{G}_{LT}^2 + (\sin\theta\cos\phi)G_{LT}^{\cos\phi})] \\
&+ |\vec{S}_{a\perp}|\Lambda_b[\cos\phi_a((\sin\theta\sin\phi)G_{TL}^{\sin\phi}) + \sin\phi_a((\cos\theta)\bar{G}_{TL}^2 + (\sin\theta\cos\phi)G_{TL}^{\cos\phi})] \\
&+ |\vec{S}_{a\perp}||\vec{S}_{b\perp}|[\cos(\phi_a+\phi_b)((\sin\theta\sin\phi)G_{TT}^{\sin\phi}) + \cos(\phi_a-\phi_b)((\sin\theta\sin\phi)\bar{G}_{TT}^{\sin\phi}) \\
&+ \sin(\phi_a+\phi_b)((\cos\theta)\ddot{G}_{TT}^2 + (\sin\theta\cos\phi)G_{TT}^{\cos\phi}) + \sin(\phi_a-\phi_b)((\cos\theta)\hat{G}_{TT}^2 + (\sin\theta\cos\phi)\bar{G}_{TT}^{\cos\phi})]\}\}.
\end{aligned}
$$

Pitonyak, Schlegel, Metz
PRD 89, 054032 (2014)

Phenomenology: Sivers and (transversity +) Collins functions from global fits

$$f_{1T}^{\perp}(x, k_T)_{[\mathrm{SIDIS}]} = -f_{1T}^{\perp}(x, k_T)_{[\mathrm{DY}]}$$

$$f_{1T}^{\perp}(x, k_T)_{[\mathrm{SIDIS}]} = -f_{1T}^{\perp}(x, k_T)_{[\mathrm{DY}]}$$

STAR – PLB 854 (2024) 138715

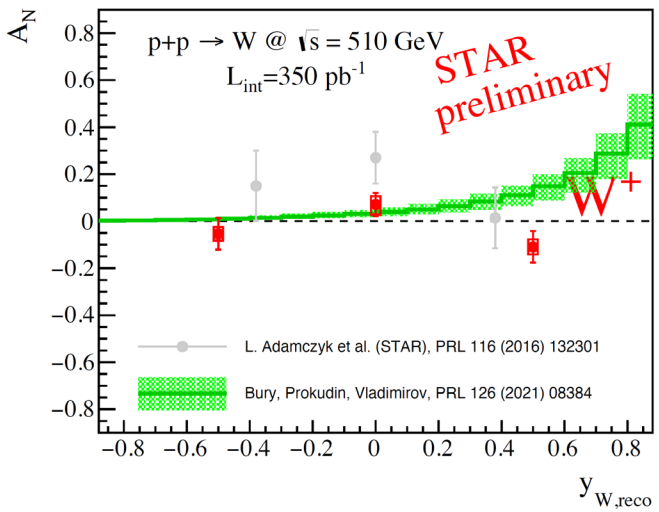

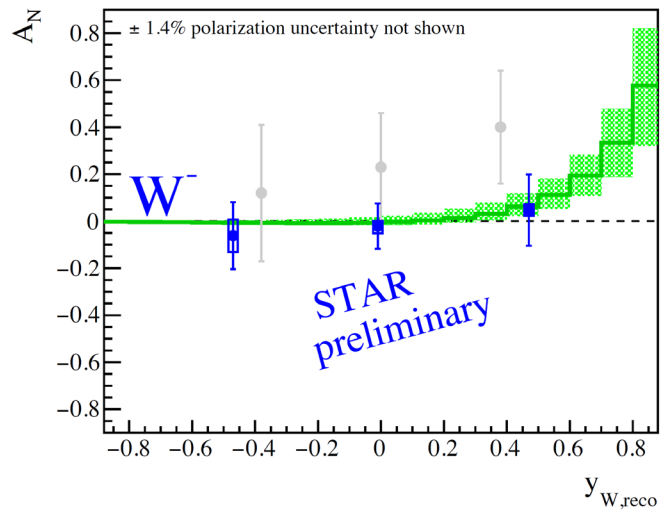

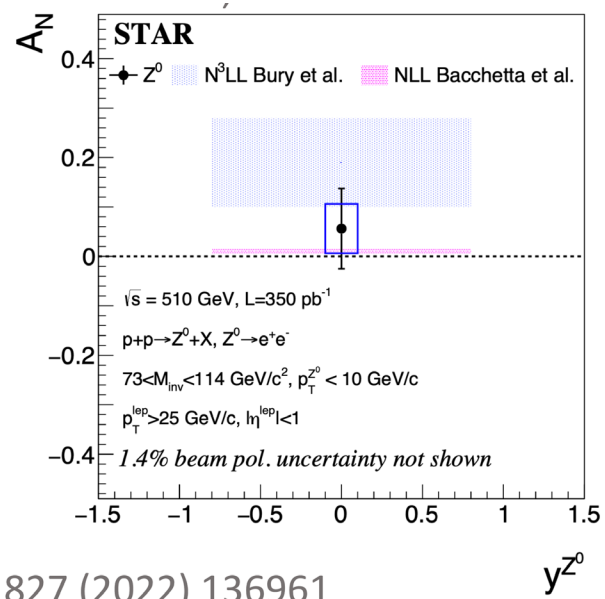

Bury et al., PRL 126 (11) (2021) 112002; Bacchetta et al.,PLB 827 (2022) 136961

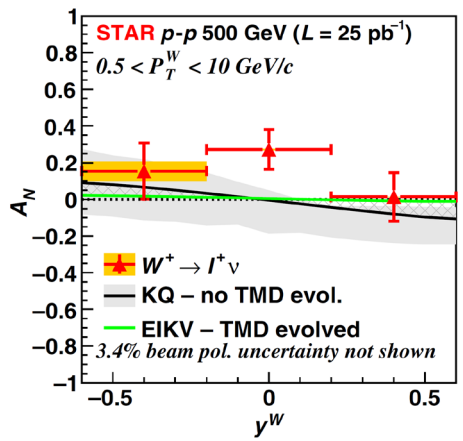

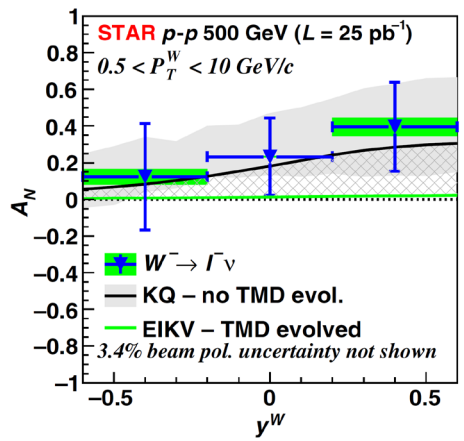

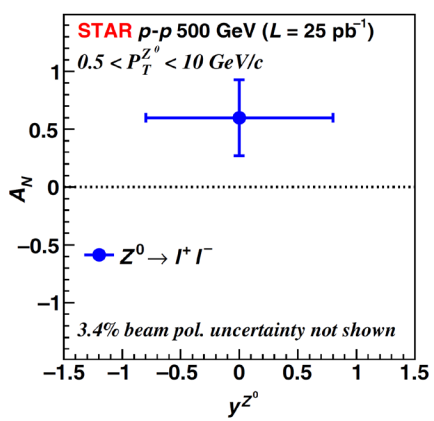

$$f_{1T}^{\perp}(x, k_T)_{[\mathrm{SIDIS}]} = -f_{1T}^{\perp}(x, k_T)_{[\mathrm{DY}]}$$

COMPASS 2312.17379 [hep-ex]

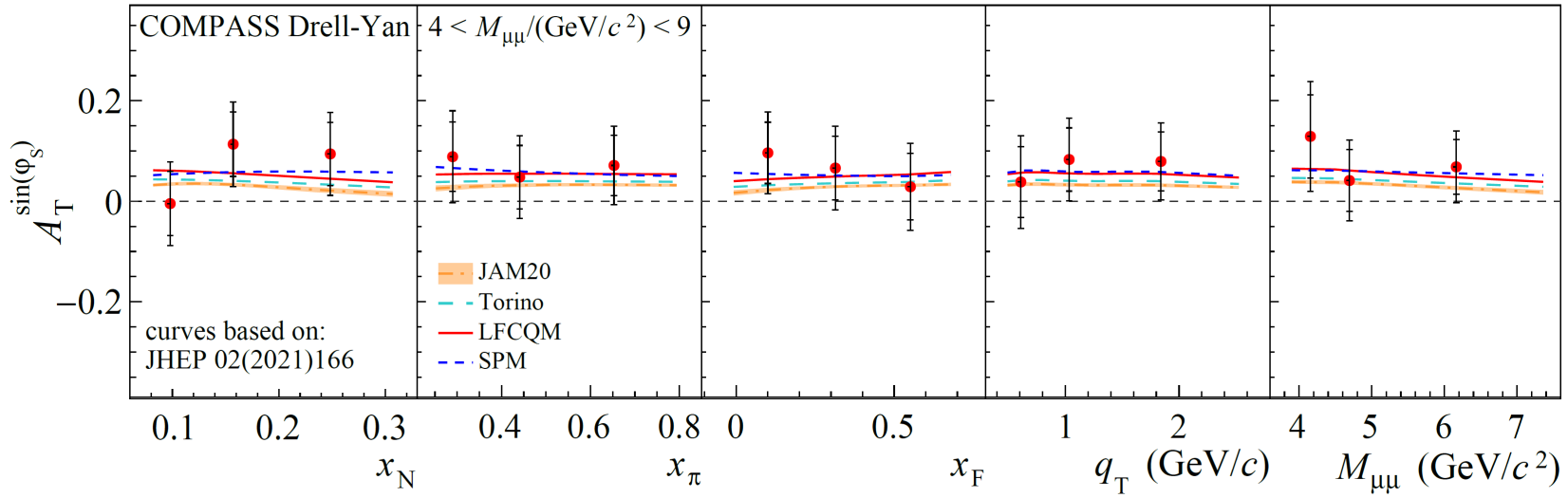

Sivers PDF -p
Unpol PDF -π

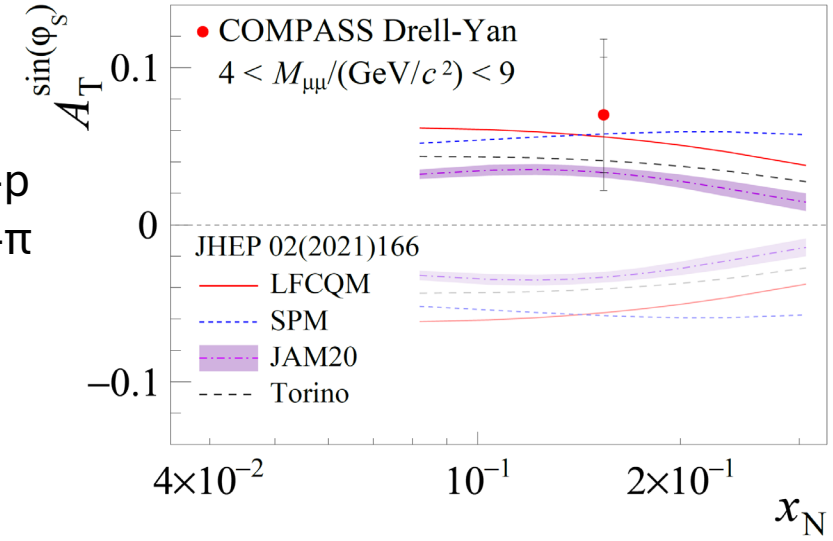

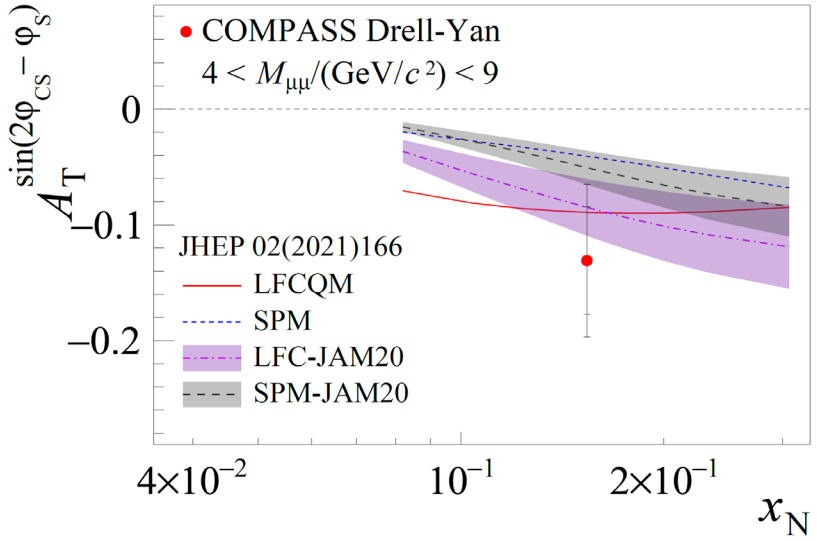

Transversity PDF - p
BM PDF – π

Bury Prokudin Vladimirov JHEP 05 (2021) 151 - N3LO e NNLO
Comparison of global SIDIS + DY fits with and without the sign change for Sivers function

	$f^{\perp}_{1T\,[DY]} = -f^{\perp}_{1T\,[SIDIS]}$	$f^{\perp}_{1T\,[DY]} = +f^{\perp}_{1T\,[SIDIS]}$
χ^2/N_{pt}	$0.88^{+0.16}_{+0.06}$	$1.00^{+0.22}_{+0.08}$
p-value (CF)	0.74	0.44
p-value 68%CI	[0.60, 0.34]	[0.28, 0.08]
p-value 68%CI (SIDIS)	[0.67, 0.42]	[0.53, 0.11]
p-value 68%CI (DY)	[0.56, 0.17]	[0.68, 0.02]

Table 5. Comparison of χ^2 and p-values between the fit with and without sign-change for Sivers function.

Extraction of Sivers function from global fits

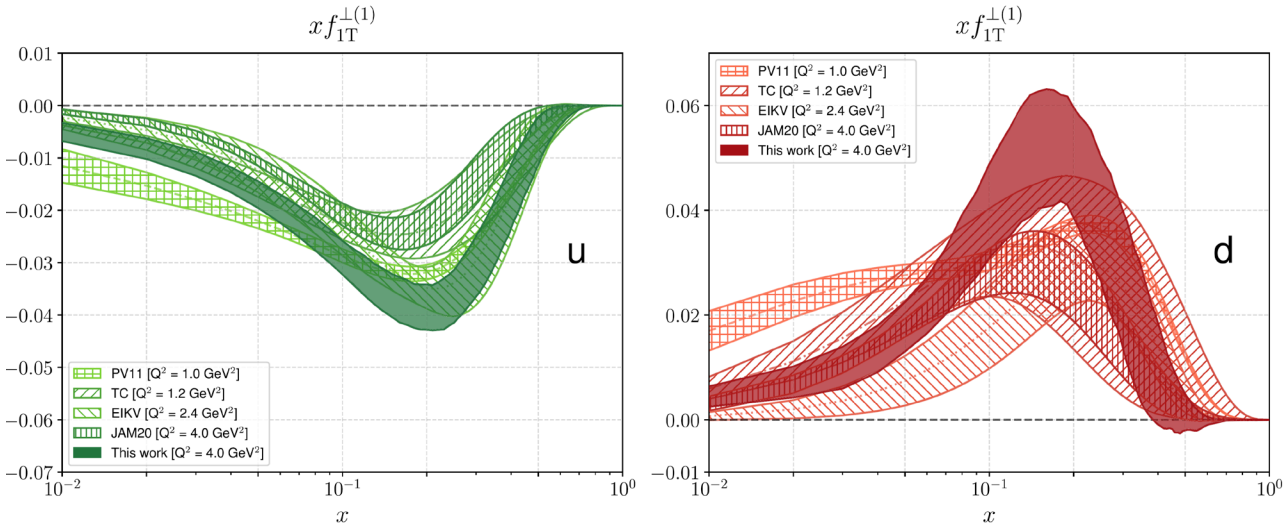

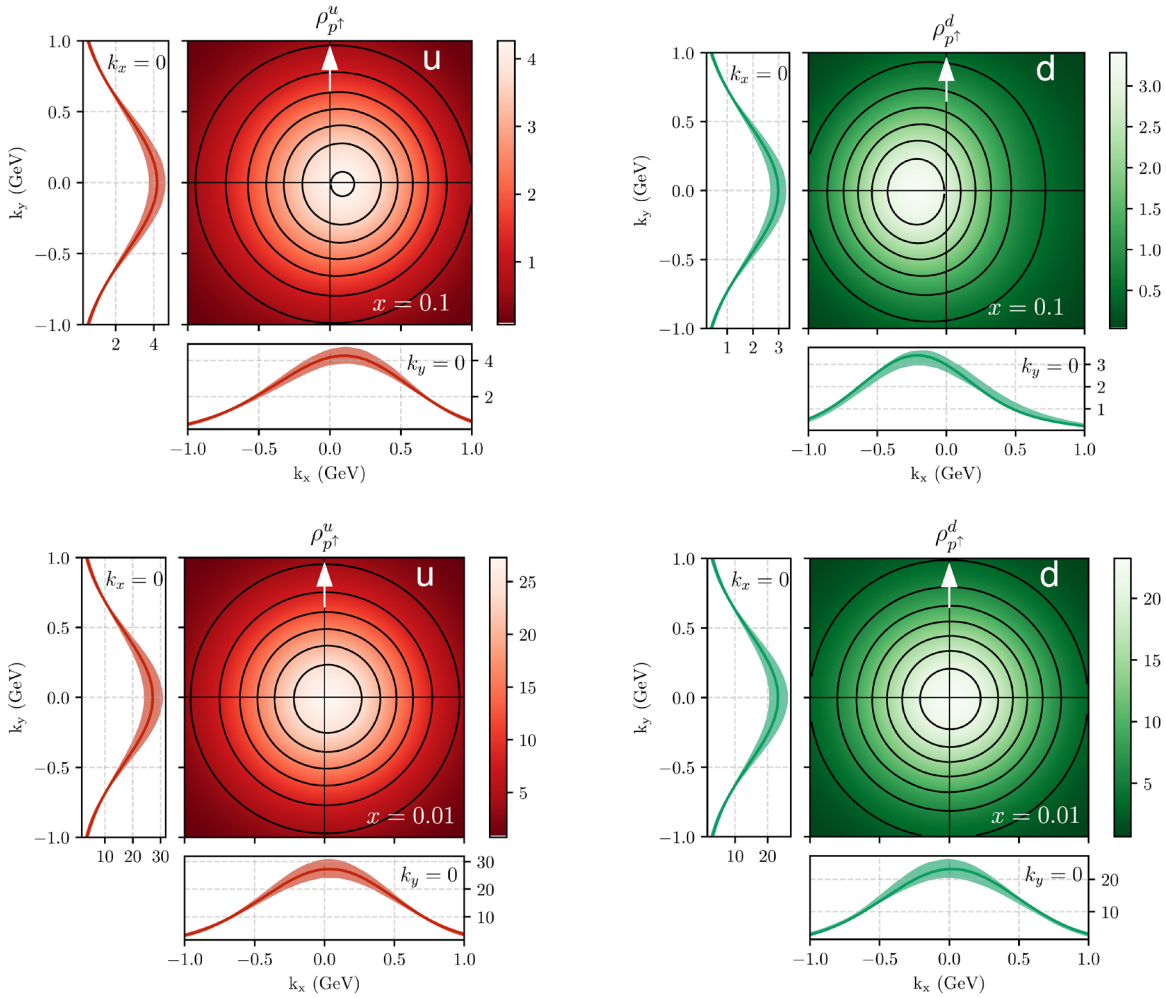

Bacchetta et al, PLB 827, 136961 (2022) – Based on PV17 global fit to unpol PDFs and FFs

JAM3D22: PRD 106, 034014 (2022)

SIDIS, DY, e^+e^- e $pp \to \pi + X$, twist-3 chiral-odd FF $\widetilde{H}$;
impact of Soffer bound and Lattice QCD tensor charge

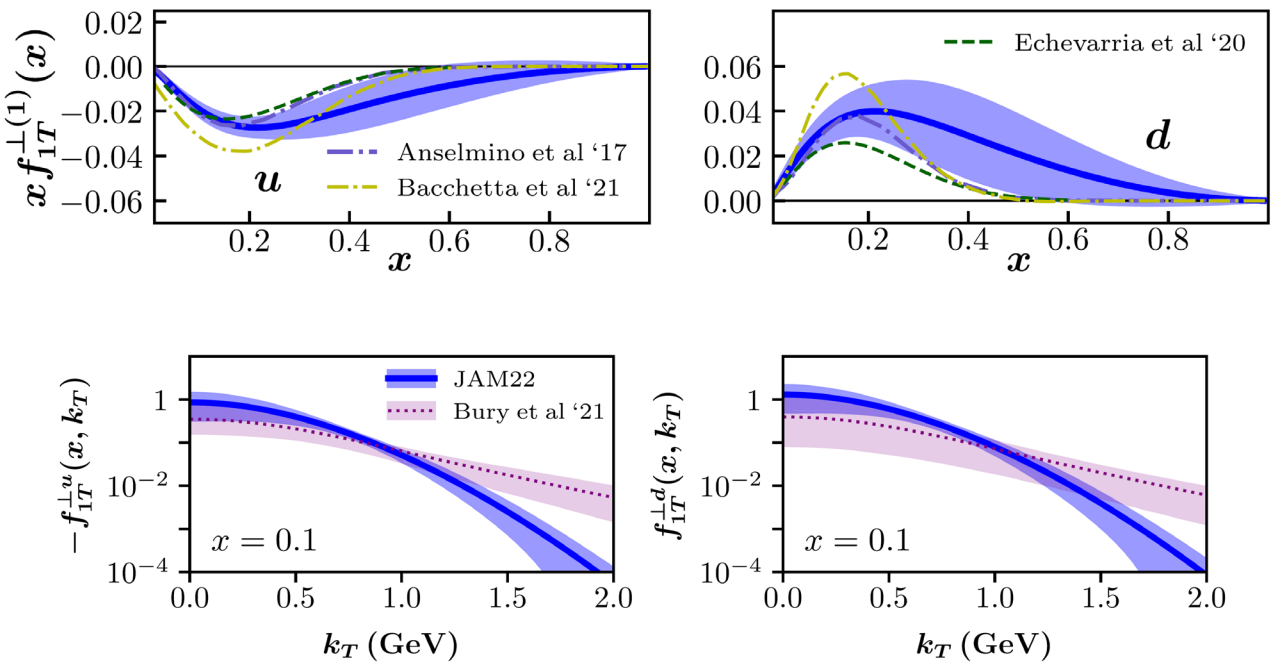

$Q^2 = 4\ GeV^2$

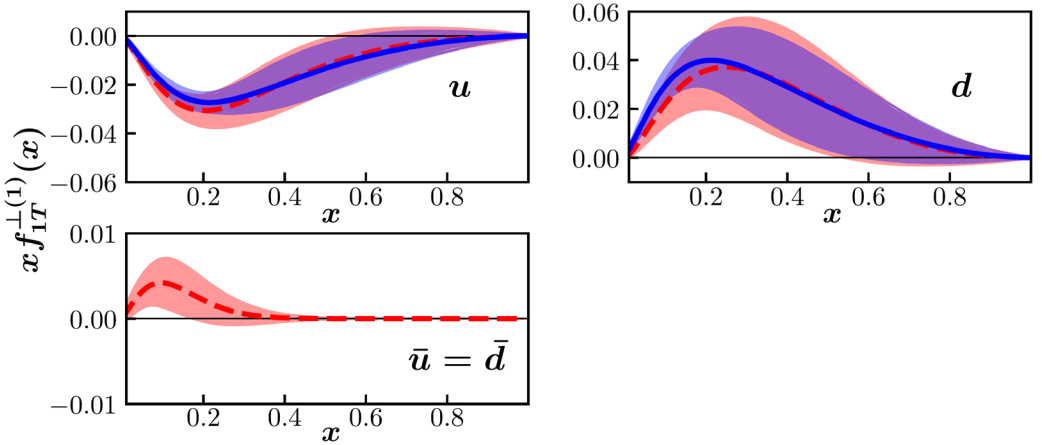

Bury, Prokudin Vladimirov JHEP 05 (2021) 151

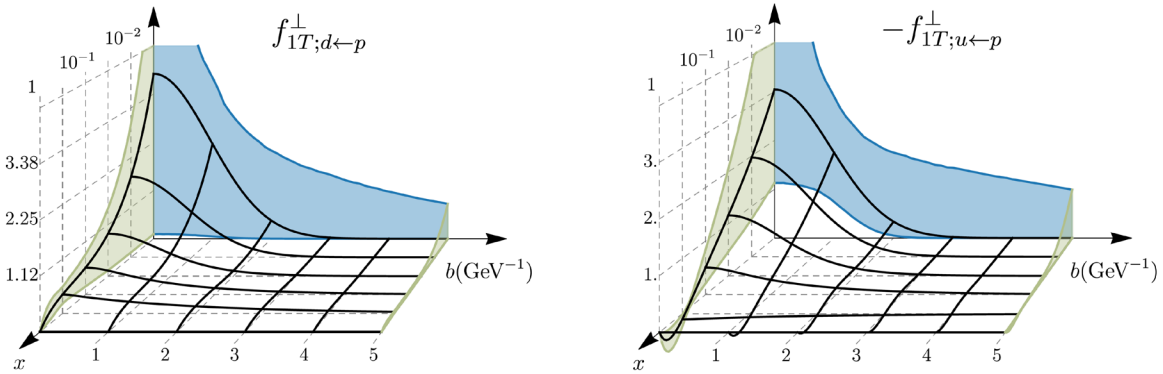

Figure 13. The (b, x)-landscape of the optimal Sivers function $f_{1T}^{\perp}(x, b)$ for d-quark (the left panel) and u-quark (the right panel). The grid shows the CF value, whereas the shaded (blue and green) regions on the boundaries demonstrate the 68%CI.

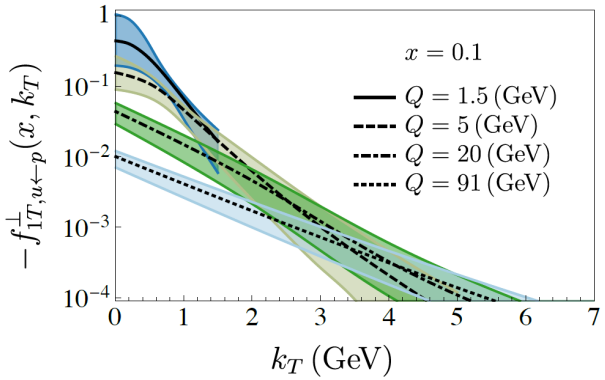

Figure 16. Sivers function in the momentum space for u quark at $x = 0.1$ as a function of k_T (GeV). The bands are the 68%CI. The calculations are performed at four different values of Q.

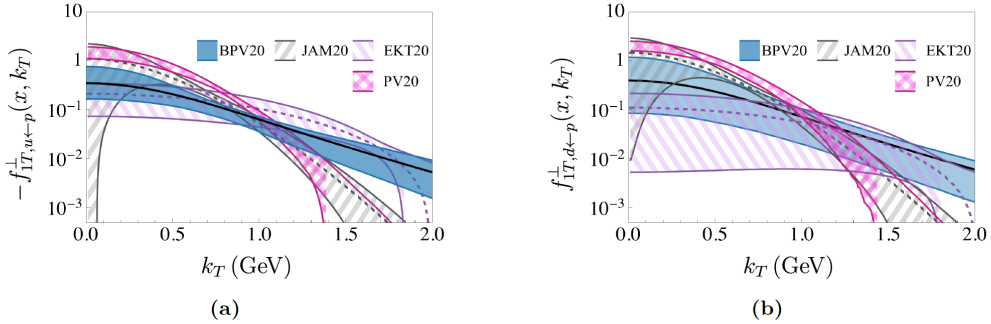

Figure 15. The comparison of the Sivers function extractions in the momentum space for u, d, quarks at $x = 0.1$ and $\mu = 2\,\mathrm{GeV}$. Our results, black solid line and the blue band, are compared to JAM20 [30] (gray dashed line with the error corridor hatched), PV20 [29] (magenta hatched region), EKT20 [31] (violet hatched region, dashed line).

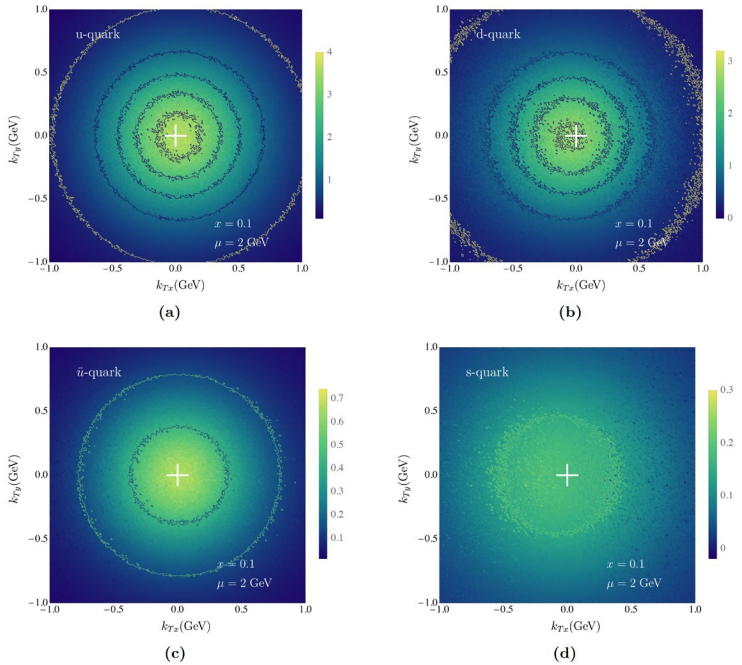

Bury, Prokudin Vladimirov JHEP 05 (2021) 151

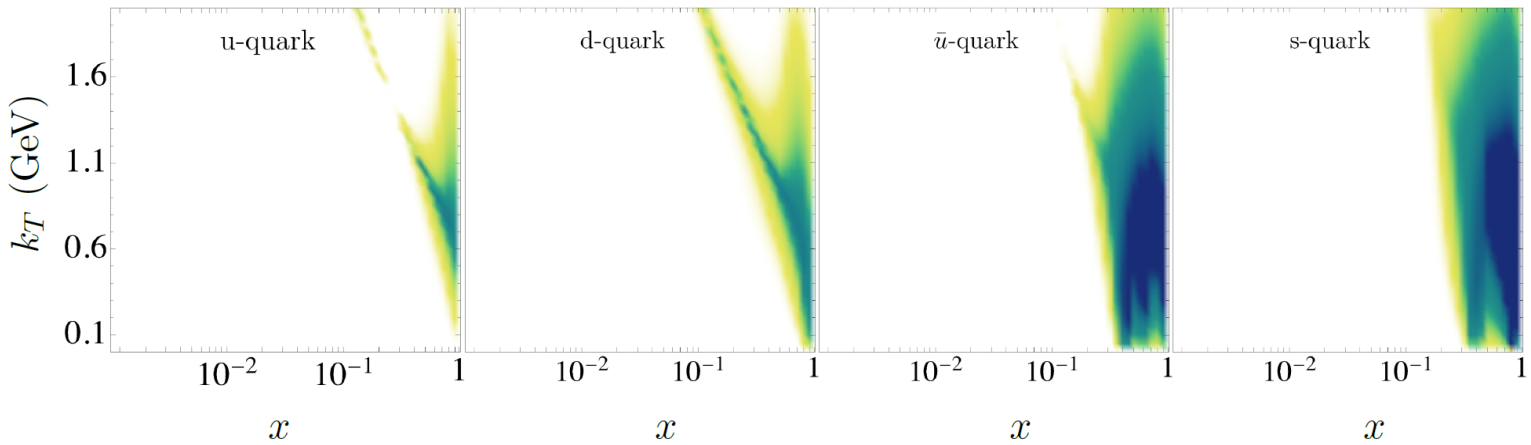

Figure 17. The function $pos(x, k_T, \mu)$ defined in eq. (4.6) at $\mu = 2$ (GeV) for u quark, d quark, $\bar{u}$ quark, s quark. The positivity constraint (4.5) is violated in the yellow-to-blue shaded region.

Echevarria, Kang, Terry, JHEP 01 (2021) 126 – NLO NNLL

Left: Only HERMES and COMPASS data for SIDIS and DY
Right: Including STAR Sivers asymmetry for W/Z (old data)

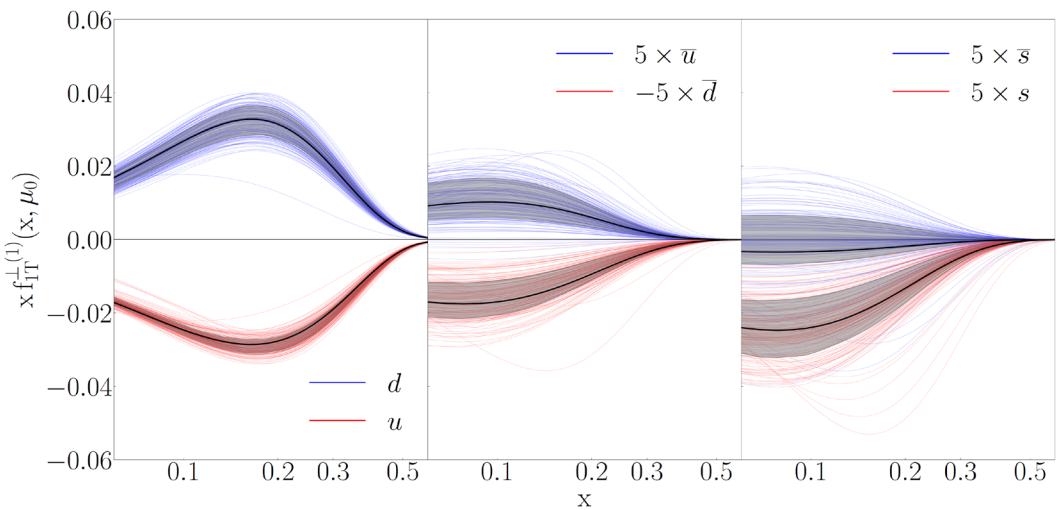

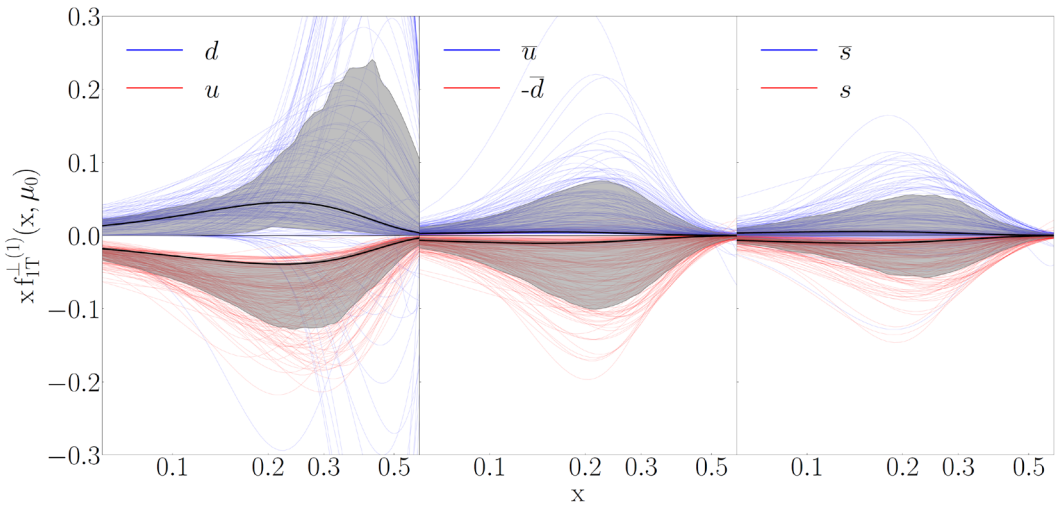

Simultaneous reweighting of TMD distributions in the (CGI)-GPM approach

M. Boglione et al. PLB 854, 138712 (2024) – 2402.12322 [hep-ph]

Updated fit of Sivers function, transversity and Collins FF from SIDIS and e+e- collisions
Reweighting using RHIC data on A_N for pions: BRHAMS charged pions, STAR neutral (full and isolated) pions

See talk by C. Flore
for details and for transversity

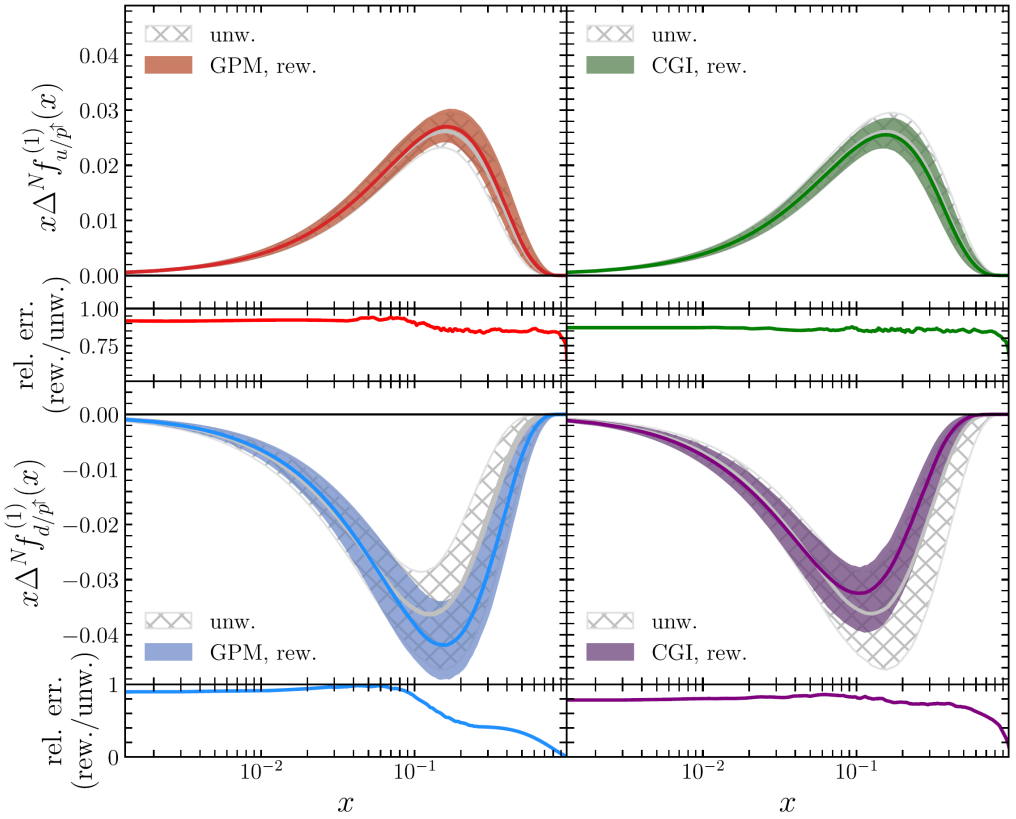

Sivers gluon distributions (f- and d-type)

$pp^{(\uparrow)} \rightarrow J/\psi + X$ - Constraining the GSF using pion and *D* meson SSA data

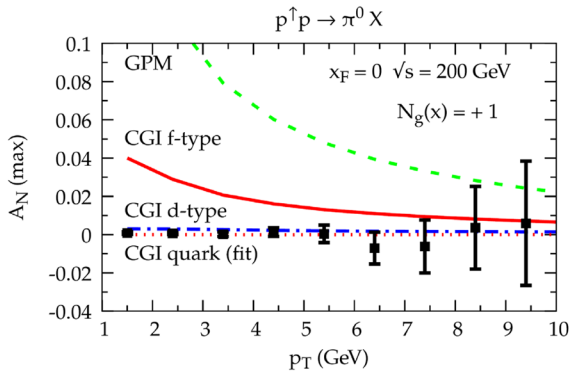

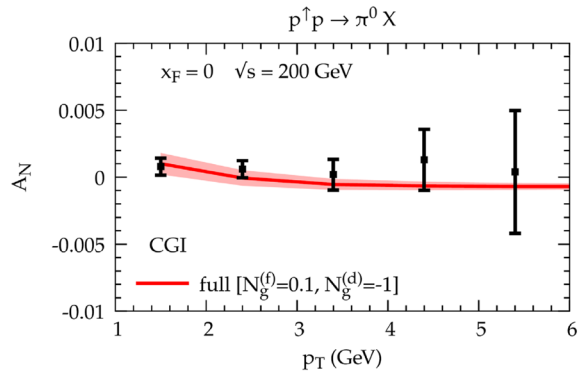

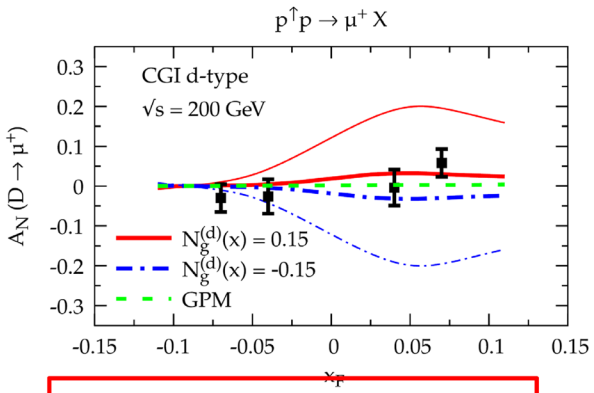

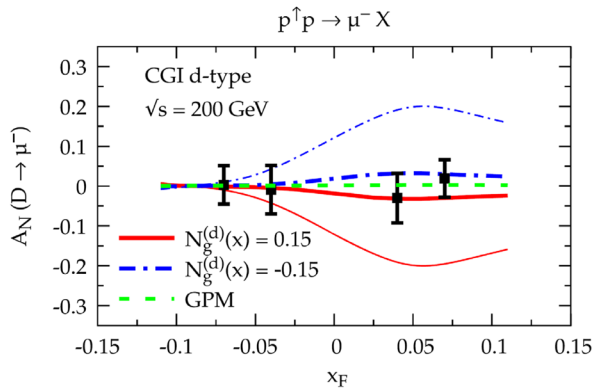

$$\mathcal{N}_g^{(d)} = -0.15 \rightarrow \mathcal{N}_g^{(f)} = +0.05$$
$$\mathcal{N}_g^{(d)} = +0.15 \rightarrow \mathcal{N}_g^{(f)} = -0.01$$

U. D'Alesio, C. Flore, FM, C. Pisano, P. Taels
PRD 99, 036013 (2019)

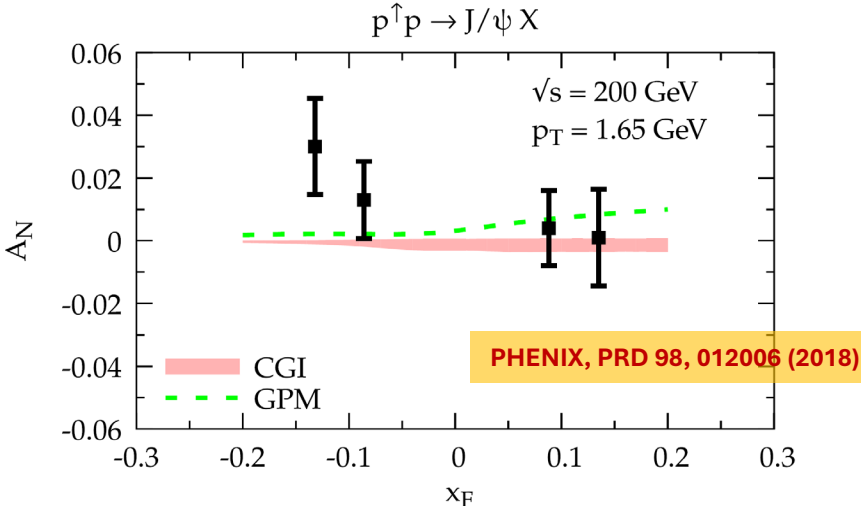

PHENIX, PRD 98, 012006 (2018)

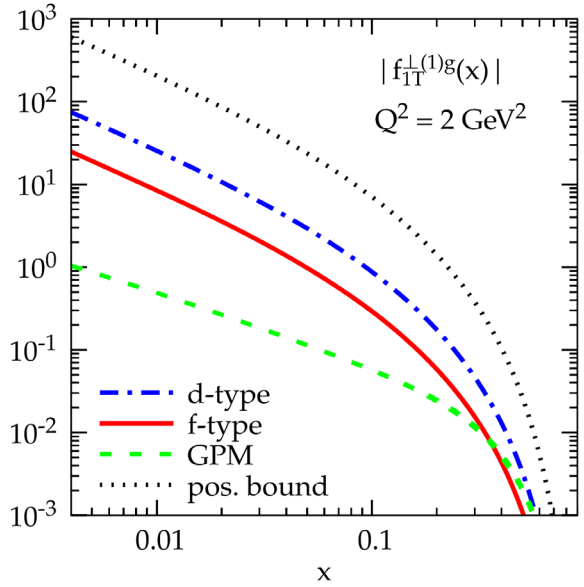

Caution: CGI-GPM factorization assumed, DGLAP-type evolution
Useful starting indications for phenomenology
See talk by D. Boer for more details on gluon TMDs, GTMDs

Bacchetta, Celiberto, Radici, T-odd gluon distributions in a spectator model, 2402.17556 [hep-ph]

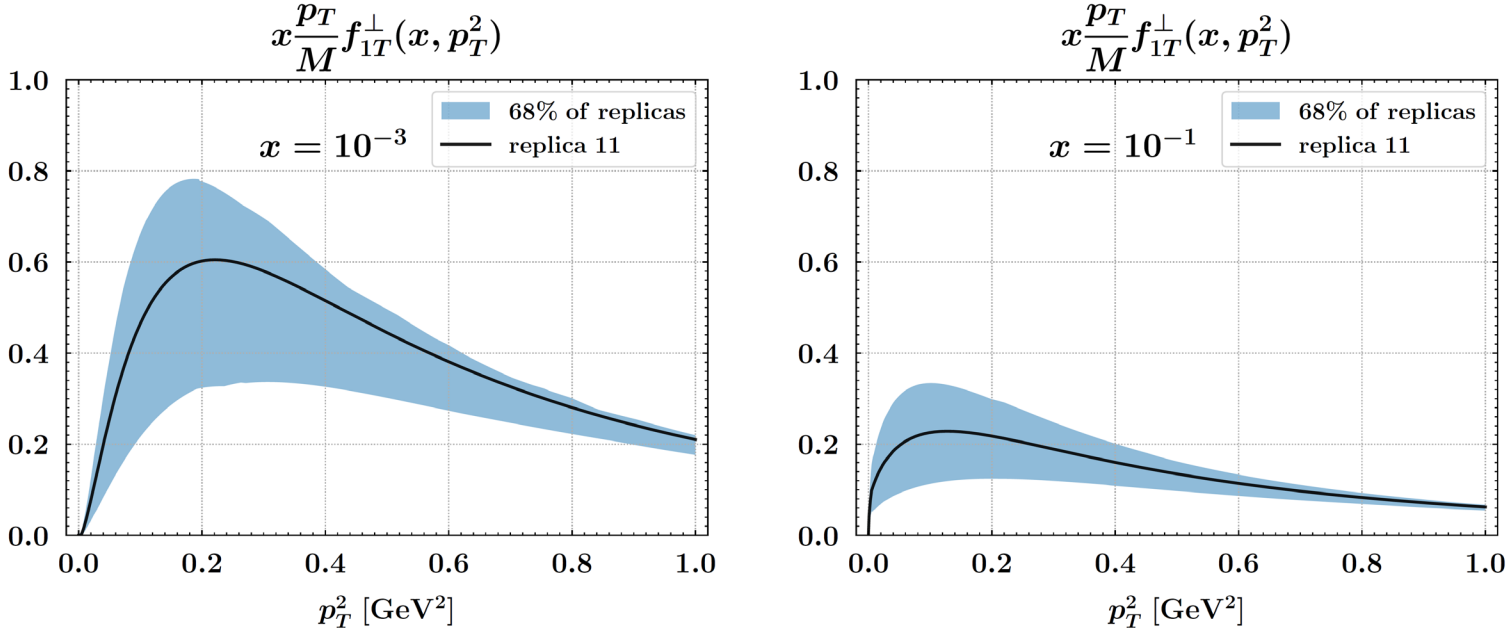

Initial scale Q_0 = 1.64 GeV

Due to model assumptions f-type and d-type differ by a calculable color factor : f-type = 5/9 d-type

Collins FF (and transversity) from SIDIS and e+e- annihilations

Kang Prokudin Sun Yuan PRD 91 (2015) & PRD93 (2016) - Figure from From TMD handbook

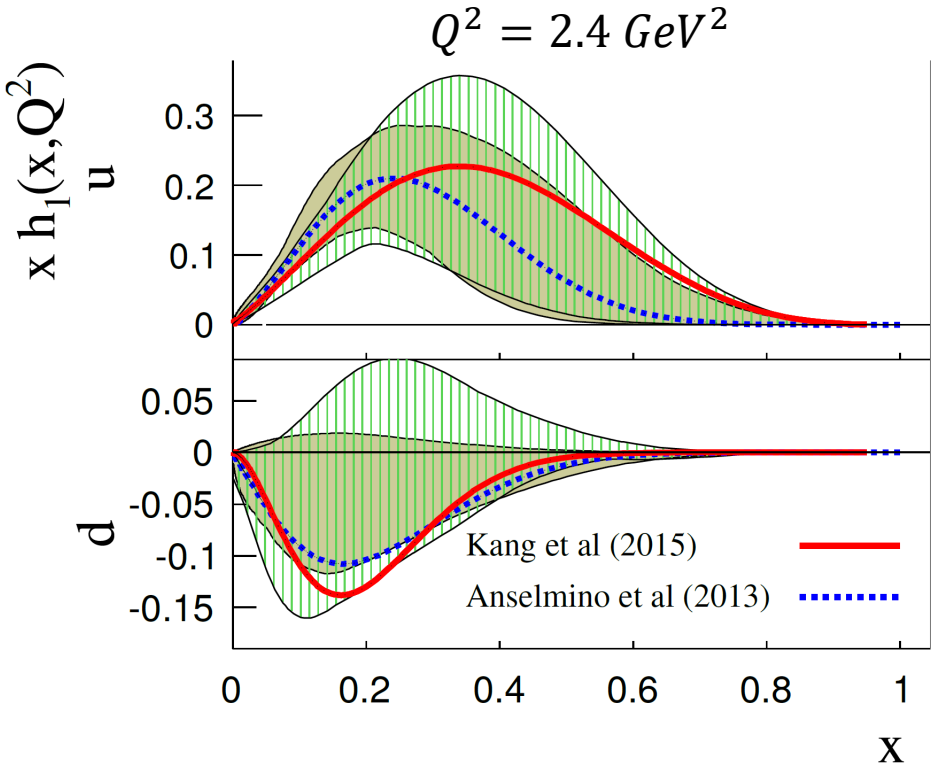

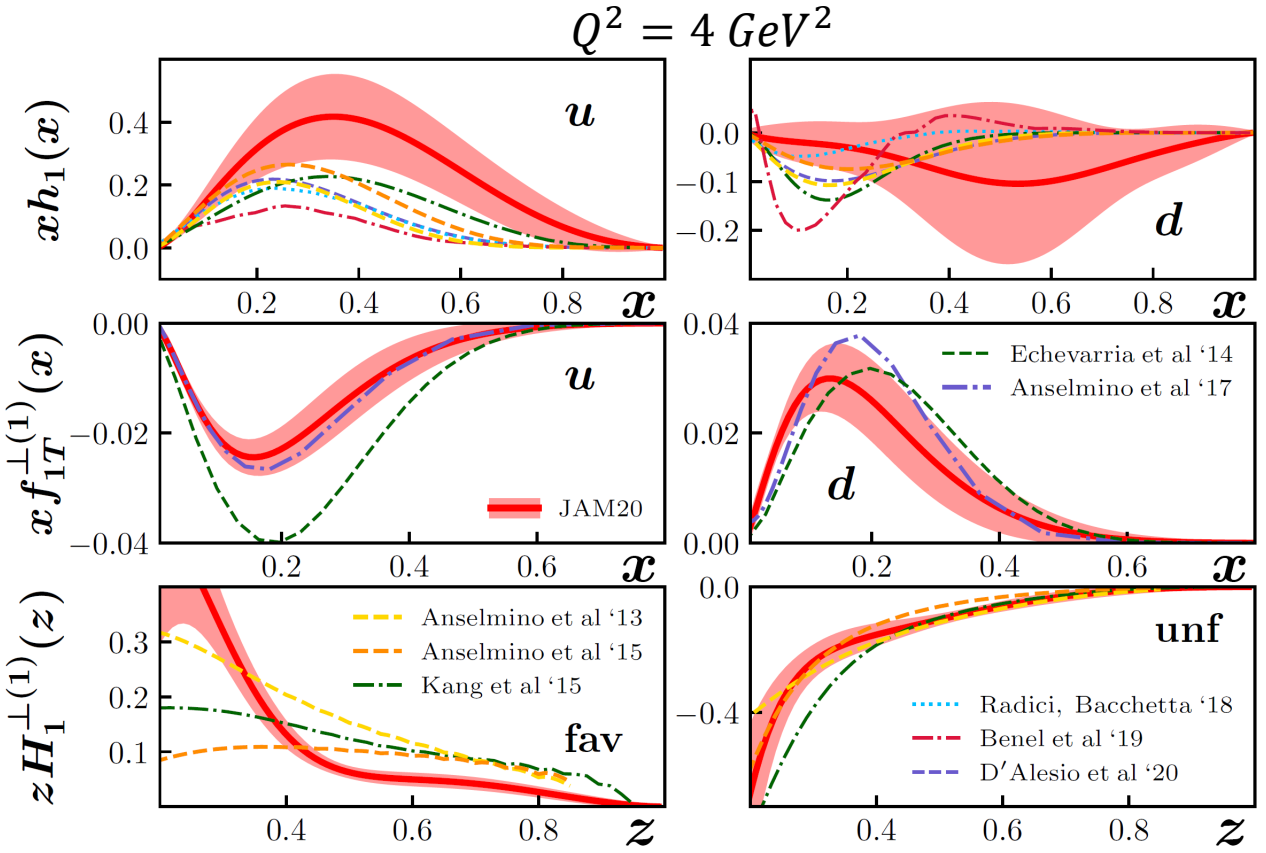

JAM3D22: PRD 106, 034014 (2022)

SIDIS, DY, e^+e^- e $pp \to \pi + X$, twist-3 chiral-odd FF $\widetilde{H}$; impact of Soffer bound and Lattice QCD tensor charge,

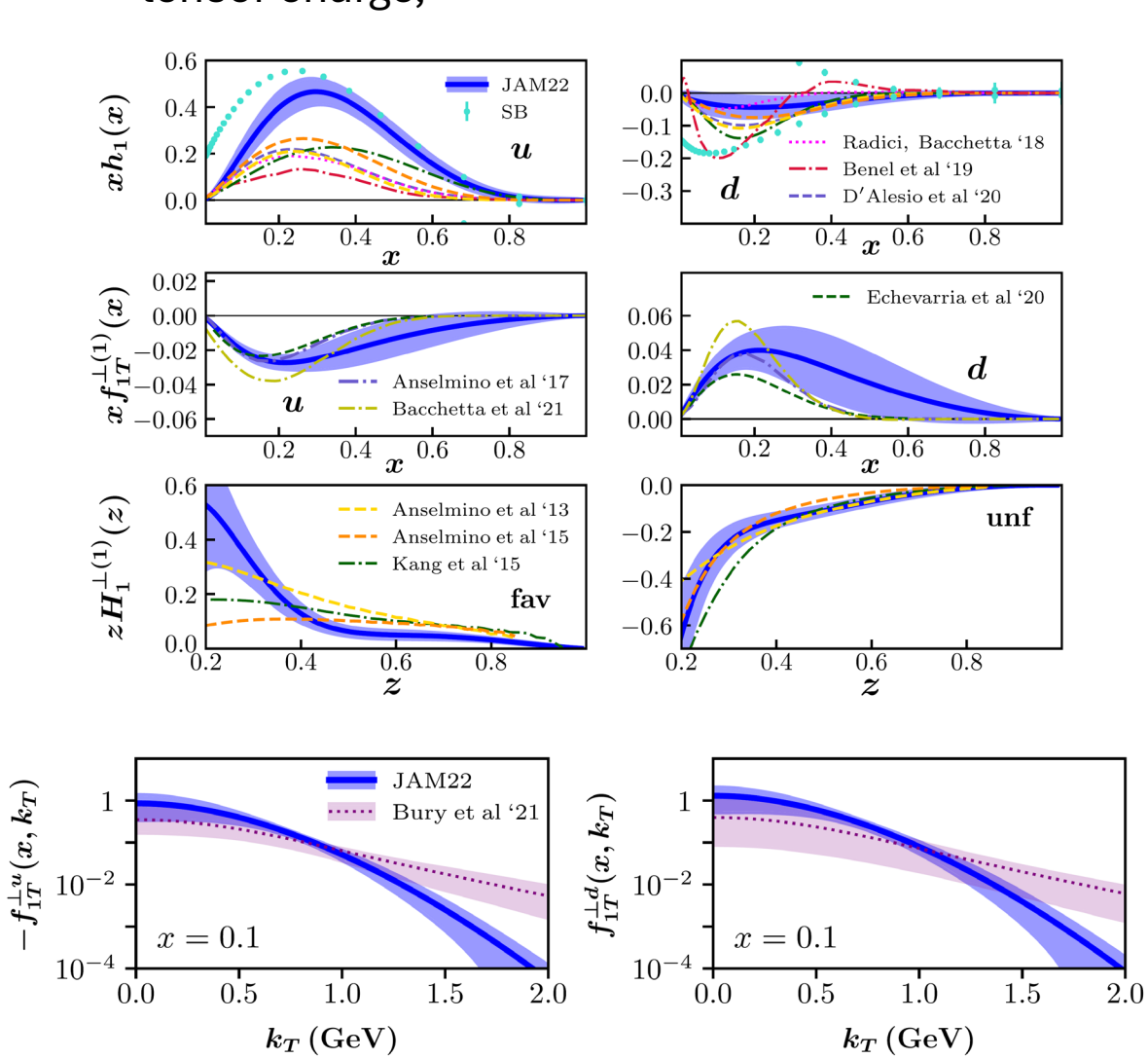

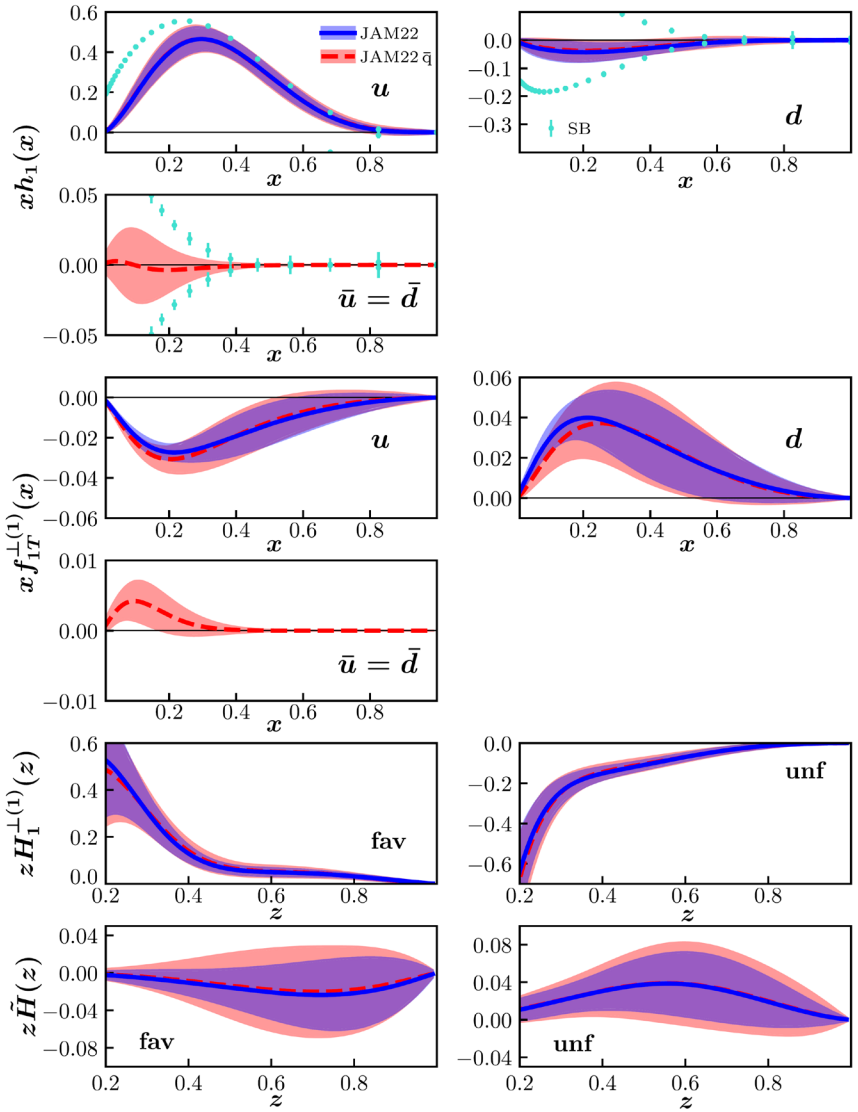

Simultaneous reweighting of TMD distributions in the (CGI)-GPM approach

M. Boglione et al. PLB 854, 138712 (2024) – 2402.12322 [hep-ph]

Updated fit of Sivers function, transversity and Collins FF from SIDIS and e+e- collisions

Reweighting using RHIC data on A_N for pions: BRHAMS charged pions, STAR neutral (full and isolated) pions

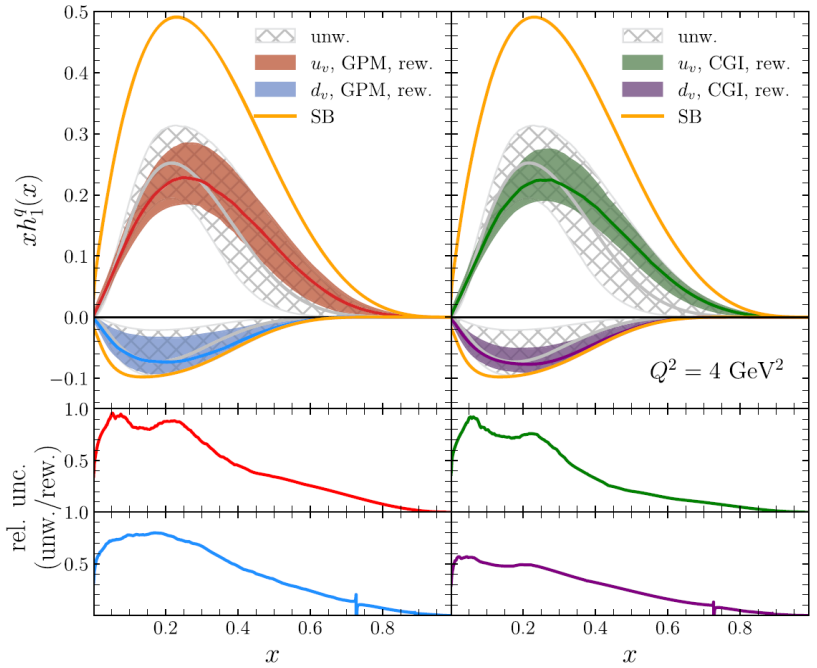

Fig. 8. Comparison of unweighted and reweighted u_v and d_v transversity functions in the GPM (left panels) and in the CGI-GPM (right panels). The corresponding Soffer bounds and the relative reduction of uncertainty (same color coding in the bottom panels) are also shown.

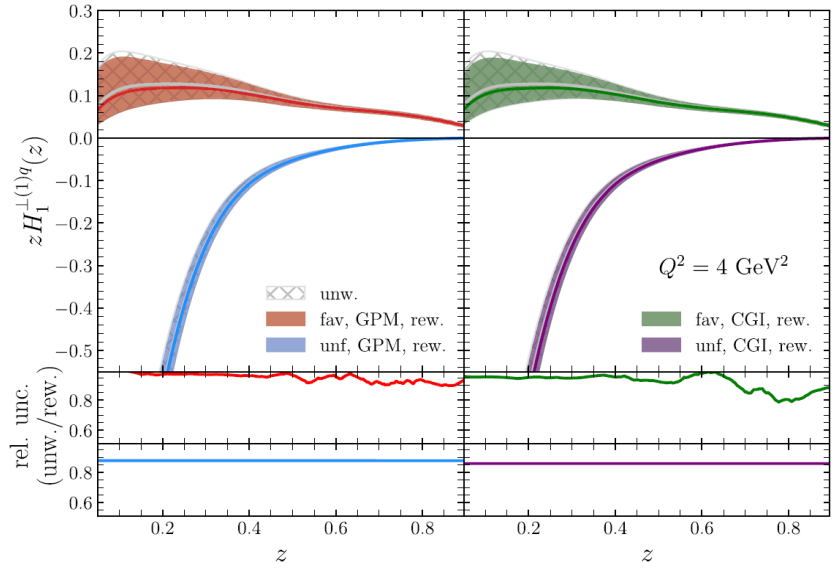

Fig. 9. Comparison of unweighted and reweighted favored (upper panels) and unfavored (lower panels) first moments of the Collins functions in the GPM (left panels) and in the CGI-GPM (right panels) at $Q^2 = 4$ GeV^2. The relative reduction of uncertainties is shown in the bottom plots.

See talk by C. Flore for more details

Collins asymmetry for hadrons inside jets in polarized pp collisions
Testing the universality of the Collins function

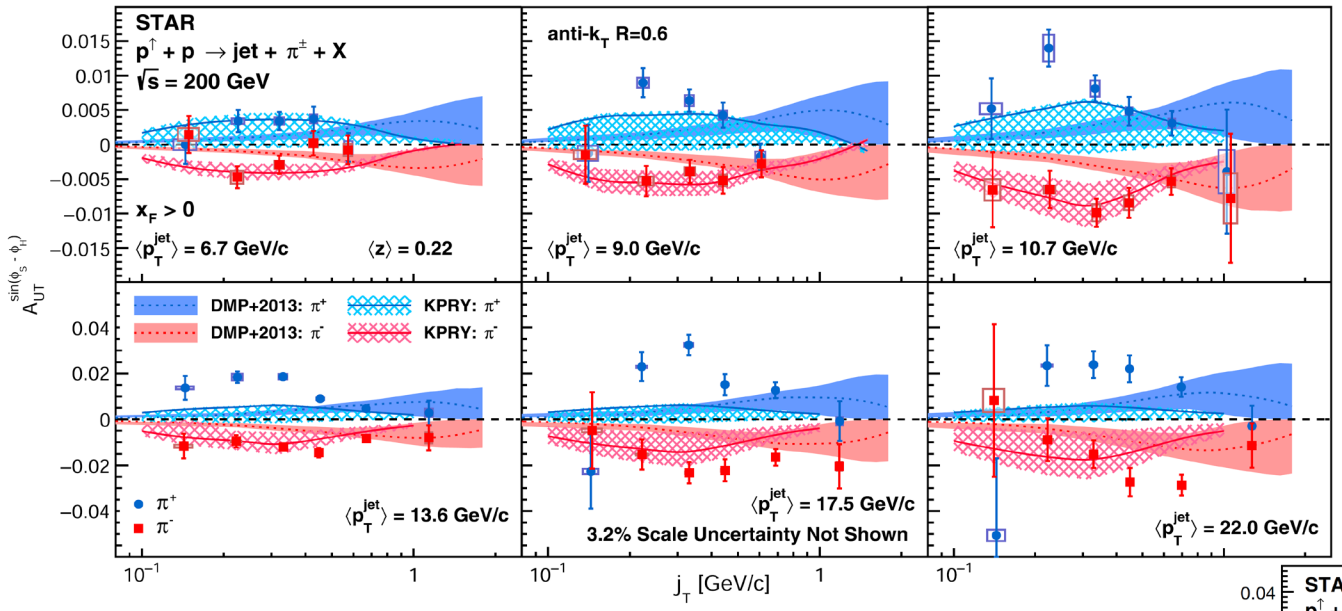

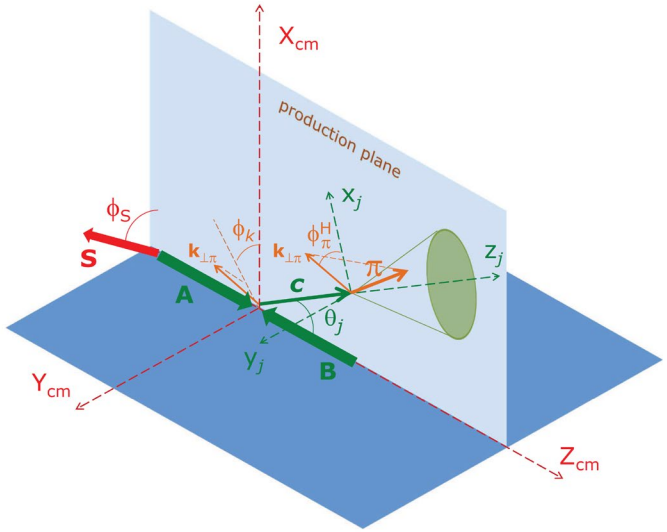

Collins Asymmetry for (charged) pions inside jet in pp collisions at 200 GeV
STAR PRD 106, 072010 (2022)

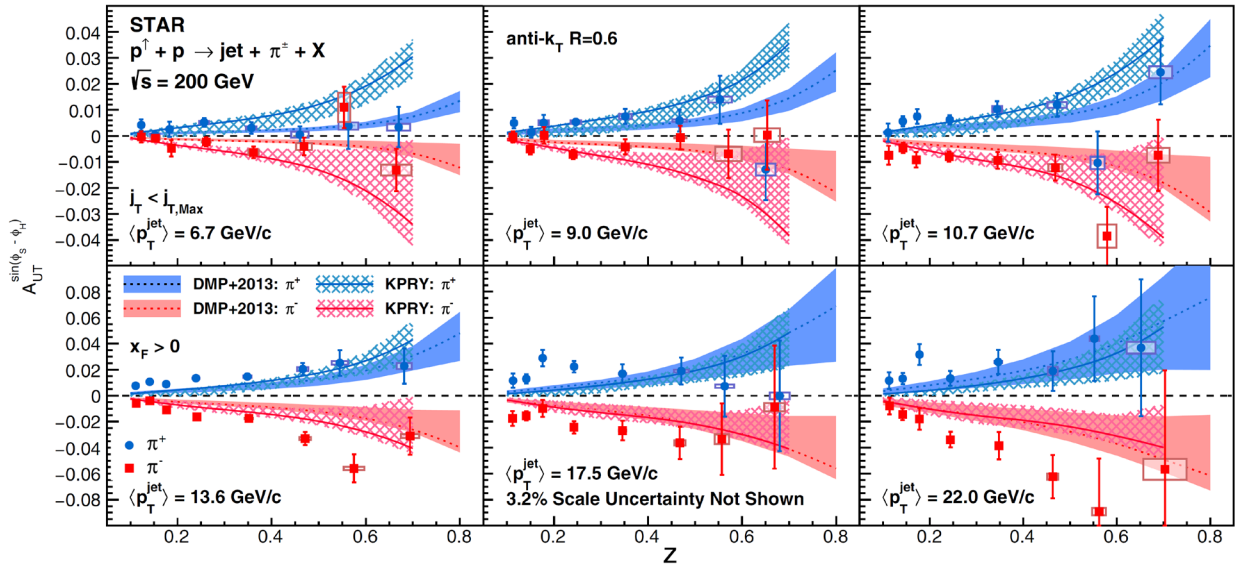

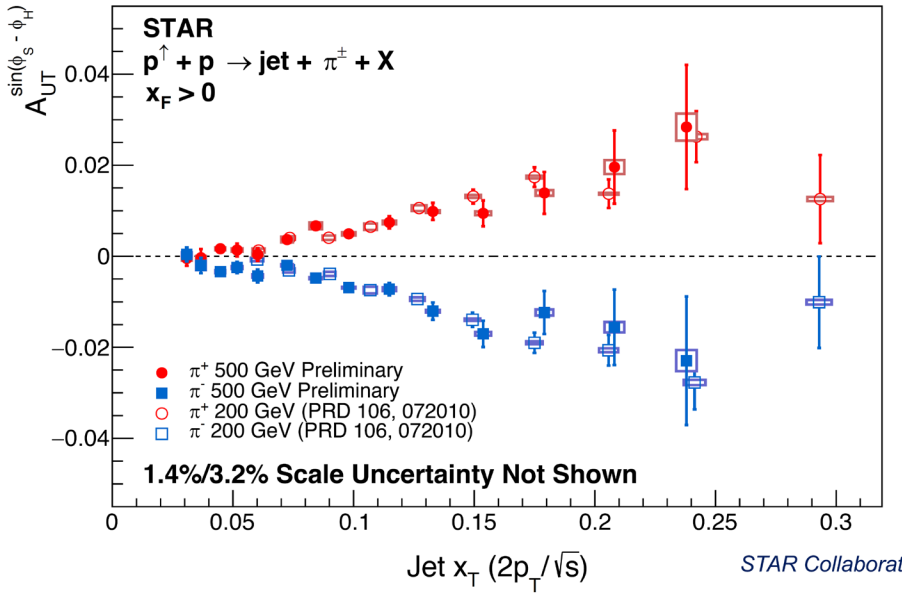

STAR Collaboration,

Collins Asymmetry for (charged) pions inside jet
in pp collisions at 500 GeV
Preliminary Xu DIS2024
Talk by B. Aboona yesterday

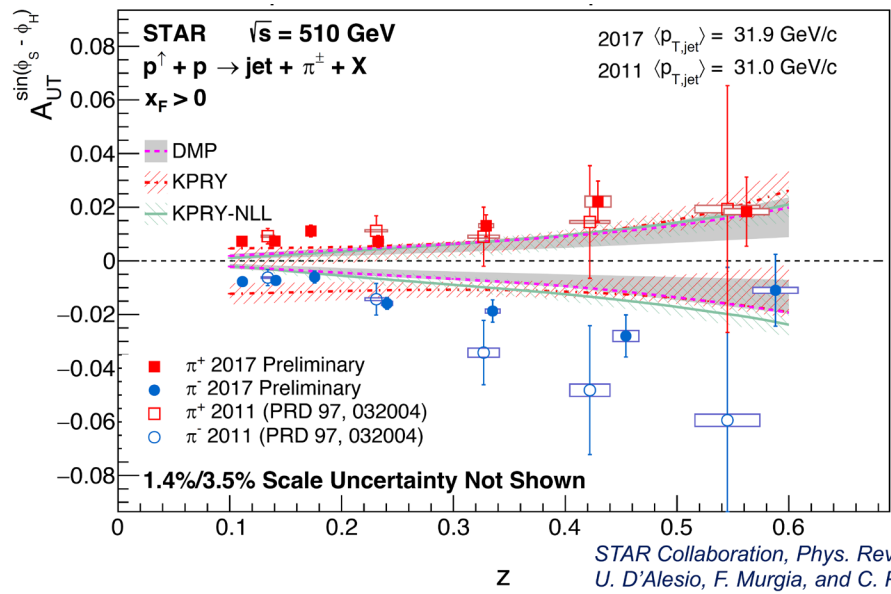

STAR Collaboration, Phys. Rev. D 97, 032004
U. D'Alesio, F. Murgia, and C. Pisano, Phys. Lett. B 773, 300
Z.-B. Kang, A. Prokudin, F. Ringer, and F. Yuan, Phys. Lett. B 774, 635

D'Alesio, FM, Zaccheddu, PRD 102 054001 (2020)
First extraction of the $\Lambda/\bar{\Lambda}$ polarizing FF from Belle data in a TMD scheme

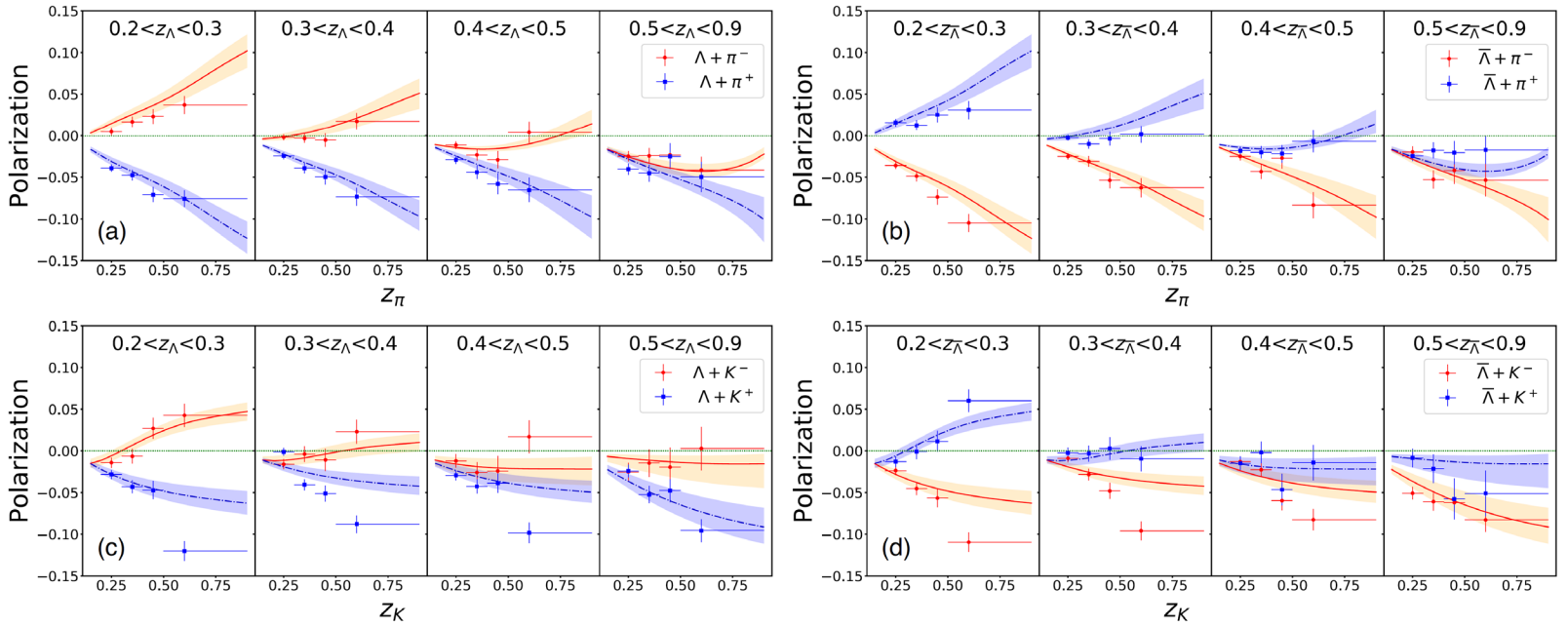

FIG. 2. Best-fit estimates, based on the full-data set, of the transverse polarization for Λ and $\bar{\Lambda}$ production in $e^+e^- \to \Lambda(\bar{\Lambda})h + X$, for $\Lambda\pi^\pm$ (a), $\bar{\Lambda}\pi^\pm$ (b), $\Lambda K^\pm$ (c), $\bar{\Lambda}K^\pm$ (d), as a function of z_h (of the associated hadron) for different z_Λ bins. Data are from Belle [8]. The statistical uncertainty bands, at 2σ level, are also shown. Data for $z_{\pi,K} > 0.5$ are not included in the fit.

See talk by M. Zaccheddu for more details and update
See also D'Alesio, Gamberg, FM, Zaccheddu:
JHEP 12 (2022) 074 – PRD 108, 094004 (2023) (TMD factorization)
PLB 851, 138552 (2024) (Λ in jet in pp collisions – STAR)

See also:
Kallos, Kang, Terry, PRD 102 096007 (2020)
Li, Wang, Yang, Lu, EPJC 81, 289 (2021)
Boer, 1007.3145 for $pp \to \Lambda$ jet + X at LHC

Boer-Mulders function

$$\frac{1}{\sigma_{DY}}\frac{d\sigma_{DY}}{d\Omega} = \frac{3}{4\pi}\frac{1}{\lambda+3}\left(1+\lambda\cos^2\theta+\mu\sin 2\theta\cos\phi+\frac{\nu}{2}\sin^2\theta\cos 2\phi\right)$$

$$F_{UU}^{\cos 2\phi_h} = C\left[\frac{2\,(\hat{\boldsymbol{h}}\cdot\boldsymbol{p}_T)\,(\hat{\boldsymbol{h}}\cdot\boldsymbol{k}_T)-\boldsymbol{p}_T\cdot\boldsymbol{k}_T}{zM_NM_h}h_1^{\perp q}H_1^{\perp q}\right]+\frac{4M_N^2}{Q^2}\,C\left[\frac{2\,(\hat{\boldsymbol{h}}\cdot\boldsymbol{k}_T)^2-\boldsymbol{k}_T^2}{2M_N^2}f_1\,D_1\right]+\ldots$$

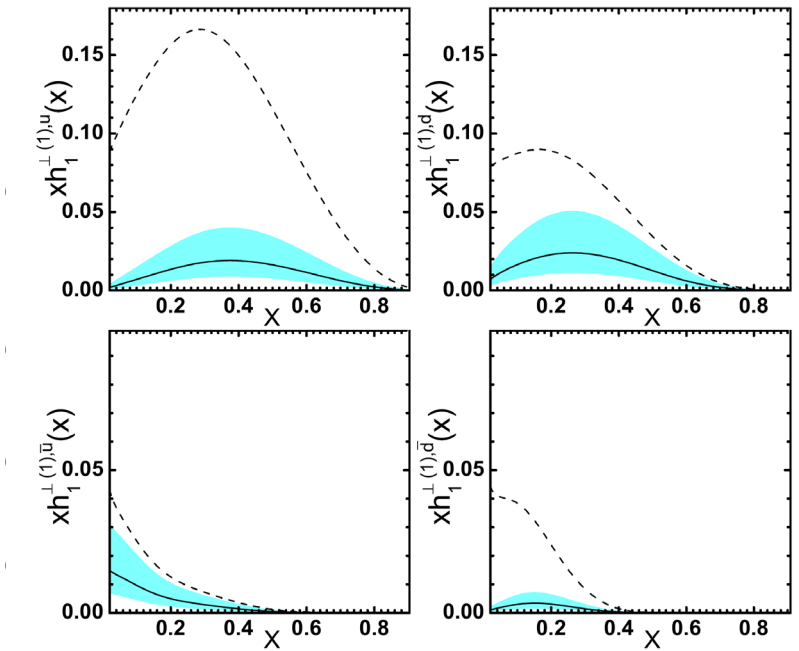

FIG. 6: The first $\boldsymbol{p}_T^2$-moments of Boer-Mulders functions for u, d, $\bar{u}$ and $\bar{d}$ quarks for $Q^2 = 1$ GeV^2 by solid lines, the shadows depict the variation ranges of $x\,h_1^{\perp(1)q}(x)$ allowed by the positivity bound. The dashed lines show $\frac{\langle p_T\rangle_{un}}{2M}x\,f_1^q(x)$. .

Lu, Schmidt, PRD 82 094005 (2010) DY data

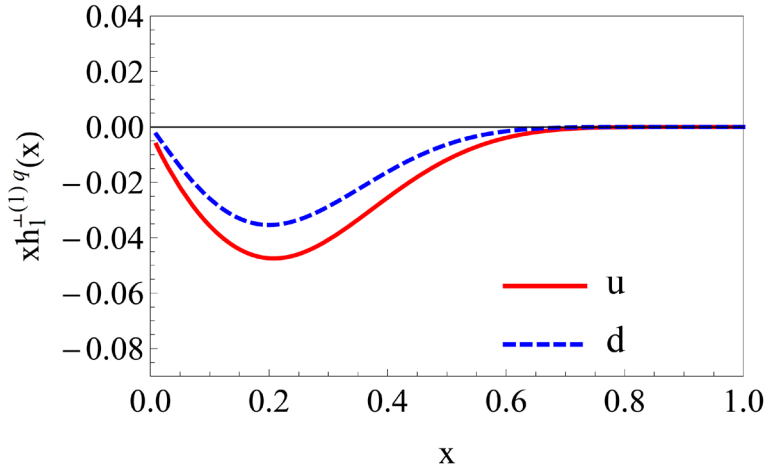

Barone, Melis, Prokudin, PRD 81 114026 (2010)
See however Barone et al, PRD 91 074019 (2015)

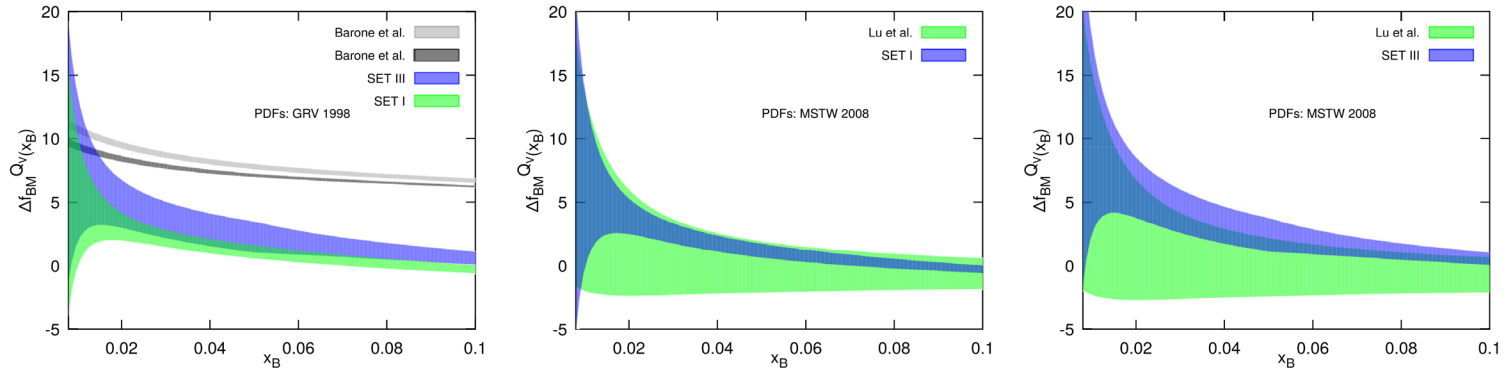

FIG. 7. Comparison of $\Delta f_{\rm BM}^{Q_V}$ for Sets I a $\Delta f_{\rm BM}^{Q_V}(x_B,Q^2) = 2\mathcal{N}_{\rm BM}^{Q_V}(x_B)Q_V(x_B,Q^2)$ gray) and [4] (dark gray) and with Lu and Schmidt—middle (Set I) and right (Set III). We use, respectively, GRV1998 [58] and MSTW2008 [59] parametrizations for the collinear PDFs.

Christova, Kotlorz,Leader, PRD 102, 014035 (2020) –SIDIS data

Worm-gear TMDs & pretzelosity

$$A_{LT}^{\cos(\phi_h-\phi_S)} = \frac{\langle 2\cos(\phi_h-\phi_S)\,\sigma_{\rm LT}\rangle}{\sqrt{1-\varepsilon^2}\,\langle\sigma_{UU}\rangle} = \frac{F_{LT}^{\cos(\phi_h-\phi_S)}}{F_{UU}}.$$

Battacharya, Kang, Metz, Penn, Pytoniak PRD 105 034007 (2022)

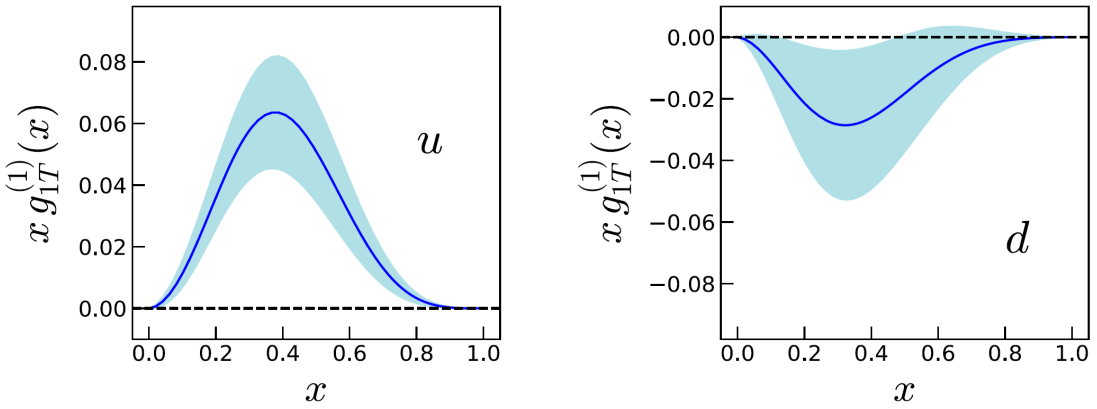

FIG. 10. Main global fit results for $xg_{1T}^{(1)}(x)$ at $Q^2 = 4$ GeV^2 for up quarks (left) and down quarks (right) obtained in the weighted χ^2 m

Worm-gear sidis fit B.Q. Ma et al: 2403.12795

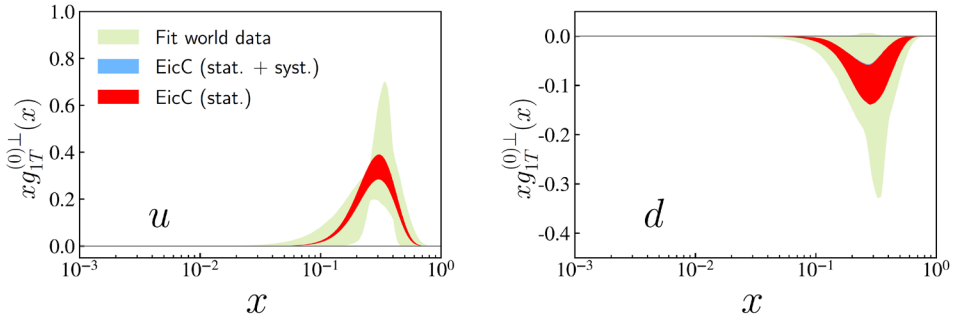

FIG. 8. The zeroth transverse moment of the worm-gear functions, $g_{1T}^{\perp(0)}(x)$ as defined in Eq. (62), for u and d quarks at the scale $Q = 2$ GeV. The uncertainty bands correspond to 68% CL estimated from the fits to 1000 replicas. The green bands are extracted distributions by fitting the world SIDIS data, the red bands are EicC projections with only statistical uncertainties, and the blue bands are EicC projections with both statistical and systematic uncertainties.

HORSTMANN, SCHÄFER, and VLADIMIROV

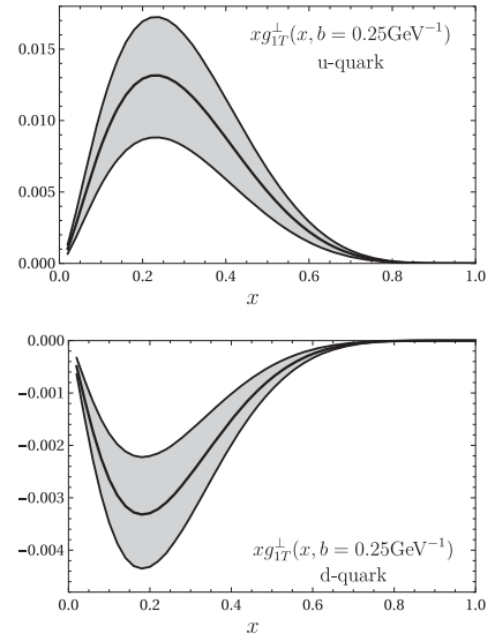

FIG. 7. The optimal wgt-function at $b = 0.25$ GeV^{-1} for u and d-quarks. The plot is shown for DSSV helicity PDF. The NNPDF plots are very similar.

Horstmann Schafer Vladimirov PRD 107 034016 (2023)

Worm-gear TMDs & pretzelosity

$$A_{UL}^{\sin 2\phi_h}(x, y, z, P_{\pi T}) = \frac{\frac{1}{xyQ^2}(1-y)F_{UL}^{\sin 2\phi_h}}{\frac{1}{xyQ^2}\left(1-y+\frac{1}{2}y^2\right)F_{UU}}.$$

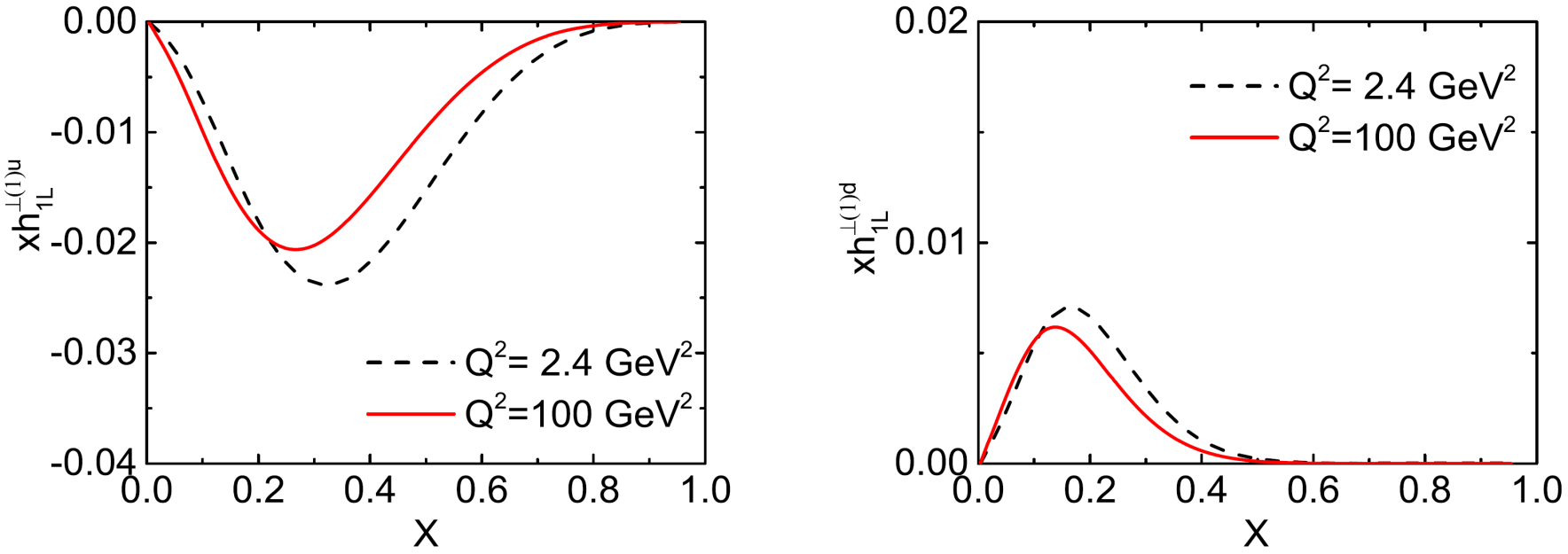

H. Li, Z. Lu, EPJC 82, 668 (2022)

Uses WW approximation and transversity parametrization from Kang et al (2015)

Notice: several models predict that $g_{1T}^{\perp}(x, k_T) = -h_{1L}^{\perp}(x, k_T)$

Pretzelosity

Lefky Prokudin PRD 91, 034010 (2015)

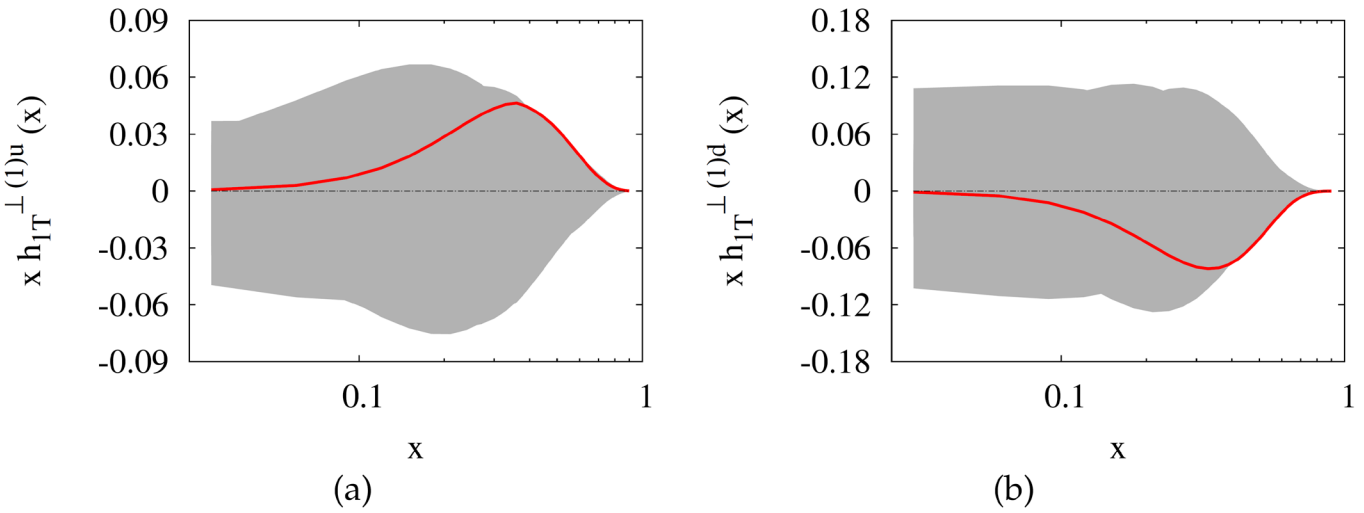

Figure 5.22: First moment of the pretzelosity distribution for up (a) and down (b) quarks at $Q^2 = 2.4$ GeV^2. The solid line corresponds to the best fit and the shadowed region corresponds to the error corridor.

See also recent work:
Liu, Ma EPJC 81, 635 (2021) (also for Boer-Mulders)
Xue, Wang, Li, Lu, PLB 820 136598 (2021) Predictions for EIC using Lefky-Prokudin extraction

Worm-gears and pretzelosity

Gabriel Santiago PRD 109 034004 (2024):
Small-x behaviour of worm-gears and pretzelosity from models:
asymptotics of the flavor non-singlet TMDs in the large-N_c limit, within linearized double logarithmic approximation (DLA)

$$g_{1T}^{\mathrm{NS}}(x \ll 1, k_T^2) \sim \left(\frac{1}{x}\right)^{0}$$

$$h_{1L}^{\perp \mathrm{NS}}(x \ll 1, k_T^2) \sim \left(\frac{1}{x}\right)^{-1}$$

$$h_{1T}^{\perp \mathrm{NS}}(x \ll 1, k_T^2) \sim \left(\frac{1}{x}\right)^{-1+2\sqrt{\frac{\alpha_s N_c}{2\pi}}}$$

Future prospects for TMD phenomenology:

- **COMPASS, AMBER**
- **RHIC (STAR, PHENIX)**
- **JLab12, SoLID, JLab20+ upgrade**
- **LHC, LHC fixed target (LHCSpin)**
- **EIC**
- **Future hadron and lepton colliders?**
- **……**

Thanks for your attention!